New Phytologist

Research

Beyond flowering time: diverse roles of an APETALA2-like transcription factor in shoot architecture and perennial traits

Yanhao Zhou[1,2,3], Xiangchao Gan[2], Natanael Viñegra de la Torre[1,2], Ulla Neumann[2] and Maria C. Albani[1,2,3]

[1]Institute for Plant Sciences, University of Cologne, Zülpicher Str. 47b, Cologne 50674, Germany; [2]Max Planck Institute for Plant Breeding Research, Carl-von-Linné-Weg 10, Cologne 50829, Germany; [3]Cluster of Excellence on Plant Sciences, "From Complex Traits towards Synthetic Modules", Düsseldorf 40225, Germany

Author for correspondence:
Maria C. Albani
Tel: +492215062380
Email: albani@mpipz.mpg.de

Received: *10 March 2020*
Accepted: *22 July 2020*

New Phytologist (2020)
doi: 10.1111/nph.16839

Key words: AP2-like, *Arabis alpina*, juvenility, perennial flowering, polycarpy, shoot architecture, TARGET OF EAT 2, vernalisation.

Summary

• Polycarpic perennials maintain vegetative growth after flowering. *PERPETUAL FLOWERING 1* (*PEP1*), the orthologue of *FLOWERING LOCUS C* (*FLC*) in *Arabis alpina* regulates flowering and contributes to polycarpy in a vernalisation-dependent pathway. *pep1* mutants do not require vernalisation to flower and have reduced return to vegetative growth as all of their axillary branches become reproductive.

• To identify additional genes that regulate flowering and contribute to perennial traits we performed an enhancer screen of *pep1*. Using mapping-by-sequencing, we cloned a mutant (*enhancer of pep1-055*, *eop055*), performed transcriptome analysis and physiologically characterised the role it plays on perennial traits in an introgression line carrying the *eop055* mutation and a functional *PEP1* wild-type allele.

• *eop055* flowers earlier than *pep1* and carries a lesion in the *A. alpina* orthologue of the *APETALA2* (*AP2*)-like gene, *TARGET OF EAT2* (*AaTOE2*). AaTOE2 is a floral repressor and acts upstream of SQUAMOSA PROMOTER-BINDING PROTEIN-LIKE 5 (AaSPL5). In the wild-type background, which requires cold treatment to flower, AaTOE2 regulates the age-dependent response to vernalisation. In addition, AaTOE2 ensures the maintenance of vegetative growth by delaying axillary meristem initiation and repressing flowering of axillary buds before and during cold exposure.

• We conclude that AaTOE2 is instrumental in fine tuning different developmental traits in the perennial life cycle of *A. alpina*.

Introduction

Plants have evolved different life history strategies. Annuals are monocarpic and set seed and senesce after flowering. Most perennials are polycarpic, being able to maintain vegetative growth from axillary meristems (AMs) and restricting senescence only to the reproductive branches (Amasino, 2009; Albani & Coupland, 2010). The distinction between annuals and perennials is underlined by several traits. Typically, most perennials have a prolonged juvenile phase during which they are not competent to respond to flower inductive stimuli. The polycarpic behaviour of perennial plants is a result of the asynchronous and differential behaviour of AMs as some commit to reproductive development, while others develop into vegetative branches or arrest growth after producing a few leaves and forming a bud (Tan & Swain, 2006; Costes *et al.*, 2014; Park *et al.*, 2017; Vayssières *et al.*, 2020). Thus, understanding the molecular mechanisms underlying the activity and fate of AMs can give insight into plant life history evolution.

Comparative studies between two Brassicaceae models, the annual *Arabidopsis thaliana* and the polycarpic perennial *Arabis alpina* have been successfully used as a tool to dissect at the molecular level the evolutionary changes driving the adoption of the annual or perennial life histories. These studies have demonstrated that several genes that regulate flowering time in *Arabidopsis thaliana* have similar and unique roles in *A. alpina* and, most importantly, that the *A. alpina* specific roles contribute to the perennial life cycle. One characteristic example is the MADS box transcription factor FLOWERING LOCUS C (FLC), a key floral repressor in the vernalisation pathway, in which prolonged cold exposure promotes flowering by stably silencing *FLC* mRNA levels in *Arabidopsis thaliana* (Michaels & Amasino, 1999; Sheldon *et al.*, 2000). The *FLC* orthologue in *A. alpina*, *PERPETUAL FLOWERING1* (*PEP1*) also regulates flowering in response to cold (Wang R. *et al.*, 2009). *pep1* mutants flower without cold exposure, whereas wild-type plants have an obligate vernalisation requirement to flower (Wang R. *et al.*, 2009). The expression pattern of *PEP1* differs from *FLC* in *Arabidopsis thaliana* so that *PEP1* mRNA levels are upregulated in axillary branches after vernalisation to maintain vegetative development and sustain the polycarpic growth habit of *A. alpina* (Wang R. *et al.*, 2009; Lázaro *et al.*, 2018). Other flowering time

regulators that typically control flowering through the age pathway, such as the *A. alpina* orthologues of *APETALA2* (*PERPETUAL FLOWERING2*, *PEP2*), *SQUAMOSA PROMOTER-BINDING PROTEIN-LIKE15* (*AaSPL15*) and *TERMINAL FLOWER1* (*AaTFL1*) also have similar and unique roles in *A. alpina* (Wang *et al.*, 2011; Bergonzi *et al.*, 2013; Hyun *et al.*, 2019; Lázaro *et al.*, 2019). PEP2, AaTFL1 and AaSPL15 determine the age at which plants become competent to cold treatment, control the duration of cold exposure required for flowering and (similar to PEP1) ensure maintenance of vegetative development in some axillary branches (Wang R. *et al.*, 2009, 2011; Bergonzi *et al.*, 2013; Hyun *et al.*, 2019; Lázaro *et al.*, 2019). The age and the vernalisation pathways are also integrated in different ways. PEP1 binds to the *AaSPL15* locus, whereas PEP2 acts upstream of PEP1 to ensure the upregulation of *PEP1* mRNA levels in axillary branches after vernalisation (Hyun *et al.*, 2019; Lázaro *et al.*, 2019).

Similarly, microRNA156 (*miR156*) that targets most SPLs in the age pathway has similar and unique roles in *A. alpina* and in *Arabidopsis thaliana*. *miR156* has similar expression patterns in both species and its accumulation is high in young seedlings and declines as plants get older (Wang J.W. *et al.*, 2009a; Bergonzi *et al.*, 2013). *miR156* in *A. alpina* also regulates flowering in the age pathway, which is evident from *A. alpina* transgenics that constitutively express *MIR156b* and do not flower in response to vernalisation, whereas the ones with suppressed *miR156* activity by target mimicry (35S:MIM156) respond to vernalisation at a younger age (Bergonzi *et al.*, 2013). The *miR156*-SPL module also regulates other traits such as plastochron, branching and AM initiation (Wang *et al.*, 2008; Wu *et al.*, 2009; Tian *et al.*, 2014; Jung *et al.*, 2016; Gao *et al.*, 2018). These additional roles of *miR156* and some of its targets have been reported in *Arabidopsis thaliana* and other species but not in *A. alpina* (Bergonzi *et al.*, 2013; Hyun *et al.*, 2019). *miR172* and its targets, *AP2* and the *AP2*-like genes *SCHLAFMUTZE* (*SMZ*), *SCHNARCHZAPFEN* (*SNZ*), *TARGET OF EAT1-3* (*TOE1-3)* are also placed in the age pathway (Aukerman & Sakai, 2003; Wu *et al.*, 2009). In *Arabidopsis thaliana*, the accumulation of *miR172* increases progressively as plants age and follows an opposite pattern to that of *miR156* (Aukerman & Sakai, 2003; Wu *et al.*, 2009). These complementary expression patterns of *miR156* and *miR172* are not observed in *A. alpina*, although one of the *miR172* targets (*A. alpina AP2*/*PEP2*) regulates age-dependent flowering in response to vernalisation (Bergonzi *et al.*, 2013; Lázaro *et al.*, 2019).

Our experiments have previously demonstrated that the *pep1-1* mutant still responds to different durations of vernalisation, suggesting that there are other repressors regulating flowering in parallel with *PEP1* (Lázaro *et al.*, 2018). Here we aimed at identifying such additional floral repressors and at characterising their contribution to the perennial life cycle. We performed an enhancer screen of *pep1-1* and identified a mutant, *enhancer of pep1 055* (*eop055*). We demonstrated that *eop055* is a *toe2* mutant in *A. alpina*. To characterise the role of AaTOE2 in the *A. alpina* life cycle and perennial traits, we introgressed the *Aatoe2* mutation in the wild-type background that has an obligate vernalisation requirement to flower and an active *PEP1* allele. We demonstrated that AaTOE2 regulates the age-dependent response to vernalisation and shoot architecture. We have previously shown that shoot architecture in *A. alpina* is organised in zones of differential bud activity and fate according to position on the plant named as V1 (zone of flowering axillary branches), V2 (zone of dormant buds) and V3 (zone of vegetative axillary branches) (Lázaro *et al.*, 2018; Vayssières *et al.*, 2020). Here we demonstrate that AaTOE2 contributes to shoot architecture by repressing flowering in axillary branches and determining the number of metamers in each zone. Many of these roles have been tailored to contribute to the perennial growth habit and have not been described for TOE2 in *Arabidopsis thaliana*.

Materials and Methods

Plant material, growth conditions and phenotypic analysis

The *pep1-1* mutant does not require vernalisation to flower and was previously obtained after the mutagenesis of the *A. alpina* accession Pajares (Wang R. *et al.*, 2009b). Here, *c.* 6000 *pep1-1* seeds were mutagenised with 0.35% ethyl methanesulphonate (Sigma) for 8–9 h. In total, 18 000 M2 seedlings (1500 M1 families) were screened in under long day (LD, 16 h : 8 h, light : dark) glasshouse and mutants that flowered earlier than *pep1-1*, named as *enhancers of pep1* (*eop*), were selected. The phenotype of mutants was subsequently confirmed in the M3 generation. The *eop055* mutant was crossed with wild-type Pajares, which requires vernalisation to flower, and an introgression line (*Aatoe2*_IL) was selected from the F2 segregating population that carried the single nucleotide polymorphisms (SNP) in *AaTOE2* and lacked the SNP in *PEP1* (responsible for the *pep1-1* phenotype). Primers used for genotyping are listed in Supporting Information Table S1. The *Arabidopsis thaliana toe2-1* mutant (SALK_065370) was obtained from the Nottingham Arabidopsis Stock Centre (NASC).

For most experiments, seeds were first stratified in darkness for 3–5 d at 4°C. Depending on the experiments, plants were grown in a long day (LD) or short day (SD) (8 h : 16 h, light : dark) glasshouse with light intensity varying from 200–500 $\mu mol\ m^{-2}\ s^{-1}$ and temperature at *c.* 22°C. Vernalisation experiments were performed in a SD growth chamber at 4°C and light intensity 14 $\mu mol\ m^{-2}\ s^{-1}$.

Flowering time experiments with *pep1-1*, *eop055* and *Arabidopsis thaliana* genotypes were performed by scoring total leaf number at flowering. *Aatoe2*_IL and Pajares plants were characterised for several traits:

(**1**) Ability to flower without vernalisation, by scoring flowering in plants growing in a LD glasshouse for up to 22 wk.

(**2**) Juvenile phase, by growing plants for 3 wk in a LD glasshouse, cold treating them for 12 wk and scoring flowering after plants were returned to LD glasshouse conditions.

(**3**) Duration of vernalisation required for flowering, by exposing 8-wk-old plants grown in a LD glasshouse to 8, 12 and 18 wk of vernalisation and scoring flowering after they were returned to LD glasshouse conditions.

(**4**) Shoot architecture, by scoring bud activity and fate in every leaf node of flowering plants exposed to 12 wk of vernalisation and subsequently grown for 8 wk in a LD glasshouse.
(**5**) Leaf initiation rate, by monitoring total visible leaf number from 2–8 wk in a LD glasshouse.
(**6**) AM initiation, by monitoring the presence or absence of a bud or an AM in each leaf node under the stereomicroscope.

All experiments were performed with at least 12 plants. Phenotypic data were analysed using Student's *t*-test.

Mapping-by-sequencing and fine mapping

A BC1F2 mapping population was created by backcrossing *eop055* to *pep1-1* and scored for flowering time in an LD glasshouse. From 450 *eop055*BC1F2 plants, 109 flowered with a similar number of leaves as *eop055*, suggesting that a single gene was segregating for flowering time. Genomic DNA was extracted from a pool of flower buds collected from 84 *eop055*BC1F2 early flowering plants. Flower buds from 48 *pep1-1* plants were also harvested for DNA extraction. Genomic DNA samples were sequenced on an Illumina HiSeq2500 (Illumina, San Diego, CA, USA) at the Max Planck Genome Center Cologne (Germany) and yielded 203 042 704 reads for *pep1-1* and 200 336 368 reads for *eop055*BC1F2. In total, 190 190 100 (93.67%) reads from *pep1-1* and 194 532 678 (95.42%) reads from *eop055*BC1F2 were aligned to the *A. alpina* V5 reference genome using Bowtie 2 (Langmead & Salzberg, 2012; Jiao *et al.*, 2017), resulting in an average coverage of 72.4 and 72.7 for the respective resequenced genome. We applied SAMtools and BCFtools to identify SNPs between samples and the *A. alpina* reference genome (Li *et al.*, 2009). SHOREmap v.3.6 was used to extract the SNPs and to visualise the allele frequency (AF) for EMS-induced mutations in *eop055*BC1F2 (Schneeberger *et al.*, 2009; Sun & Schneeberger, 2015). SNPs with a quality score lower than 40 were filtered out from the *eop055*BC1F2 data. In addition, homozygous SNPs in the *pep1-1* resequencing data were used for background correction and were also filtered out from the *eop055*BC1F2 data.

To fine map the *EOP055* locus, 11 molecular markers were developed based on SNPs detected by the resequencing data to be polymorphic between *eop055*BC1F2 and *pep1-1*. For fine mapping, we screened 503 BC1F2 plants. Primers used for fine mapping are listed in Table S1. The raw and processed resequencing data have been submitted to GenBank under the accession no. GSE145718.

Plasmid construction and plant transformation

To generate the *pAaTOE2*:g*AaTOE2 eop055* transgenic lines, 4128 bp upstream of the translational start of *AaTOE2* and 3672 bp spanning *AaTOE2* (from the ATG up to 776 bp downstream of its translational stop) were combined separately into the GATEWAY cloning vector pDONR207 (Invitrogen, Darmstadt, Germany) using the polymerase incomplete primer extension (PIPE) method (Klock *et al.*, 2008). The generated 7.8 kb *AaTOE2* DNA construct was then recombined into the pEarlyGate301 binary vector and transformed into the *eop055* mutant. For construction of *35S:AaTOE2* and *35S:Aatoe2*, *AaTOE2* cDNA was amplified from *pep1-1* and *eop055*, respectively. cDNAs were subsequently cloned into the destination vector pLEELA containing a double Cauliflower Mosaic Virus (CMV) 35S promoter and transformed into the *Arabidopsis thaliana toe2-1* mutant. Primers used for plasmid constructions are listed in Table S1. Plant transformation in *A. alpina* and *Arabidopsis thaliana* was performed using the *Agrobacterium*-mediated floral dip method (Clough & Bent, 1998).

RNA extraction and expression studies

For main shoot samples, apices from 12–50 plants per sample were combined for all experiments. For V3 bud samples, buds from leaf axils 21–26 were harvested under a stereomicroscope from 24–48 plants per sample. Total RNA was isolated from plant tissues using the miRNeasy Plant Mini Kit (Qiagen, Hilden, Germany) and subjected to DNase treatment using DNA-free DNase (Ambion). For normal qRT-PCR reactions, 1 μg of total RNA was used as a template for the synthesis of cDNA by reverse transcription with SuperScript II Reverse Transcriptase (Invitrogen) and oligo(dT) (18) primer. For qRT-PCR of miRNA reactions, 200 ng of total RNA was used for reverse transcription using specific key primers. Quantitative PCRs to follow gene expression were carried out as described in Lázaro *et al.* (2019) and for miRNAs as described in Bergonzi *et al.* (2013). For each sample, three technical replicates and three biological replicates were analysed. Transcript accumulation of selected genes in *A. alpina* samples was normalised using the *A. alpina PROTEIN PHOSPHATASE 2A* (*AaPP2A*) and *RAN GTPASE 3* (*AaRAN3*) and in *Arabidopsis thaliana* samples using *ACTIN*. qPCRs for *miR156* and *miR172* were normalised using *AasnoR101*. Expression data were analysed using Student's *t*-test. Primers used in this analysis are listed in Table S1.

RNA-seq

For transcriptome analysis we dissected main shoot apices and V3 buds from *Aatoe2*_IL and wild-type plants as described above in three biological replicates per sample. RNA was extracted using the miRNeasy Plant Mini Kit (Qiagen, Hilden, Germany) and subjected to DNase treatment using DNA-free DNase (Ambion). PolyA enrichment, library preparation and sequencing were performed at the Max Planck Genome Center, Cologne (Germany). PolyA RNA was isolated from 1 μg of total RNA using NEBNext Poly(A) mRNA Magnetic Isolation Module (New England Biolabs, Frankfurt am Main, Germany) and used for library construction with NEBNext Ultra Directional RNA Library Prep Kit for Illumina (New England Biolabs). Sequencing was performed on an Illumina HiSeq 3000 system with 1 × 150-bp single-read lengths.

Sequencing reads were mapped and aligned to the reference genome (*A. alpina* V5) using STAR software (Dobin *et al.*, 2013). Raw read counts per gene were quantified with HTSeq v.0.5.4p1. The differentially expressed genes with more than a two-fold change and an adjusted *P*-value below 0.05 were

obtained using DESeq2 (Anders & Huber, 2010) and selected for further analysis. The raw and processed data for RNA-seq analysis have been submitted to GenBank under the accession no. GSE145718.

Gene Ontology (GO) enrichment analysis was performed using the DAVID resource (Huang *et al.*, 2008). DEGs with homologues in *Arabidopsis thaliana* were used as input data for GO analysis. GO terms with a Benjamini-Hochberg adjusted *P*-value lower than 0.05 were plotted using the R-based graphical tool BACA (Fortino *et al.*, 2015).

Scanning electron microscopy (SEM) and light microscopy

For scanning electron microscopy, samples were fixed overnight at 4°C in 10 mM phosphate buffer containing 4% glutaraldehyde solution (pH 7.4), rinsed twice with 10 mM phosphate buffer and dehydrated in a graded ethanol series. Samples were critical point dried using a Leica CPD300 dryer (Leica Microsystems, Wetzlar, Germany) and mounted onto stubs with double-sided adhesive carbon tabs. Afterwards they were sputter-coated with platinum (Polaron SC 7640), images were taken with a Zeiss Supra 40VP SEM (Carl Zeiss, Jena, Germany).

For light microscopy, axillary buds from leaf axils 21 and 23 were fixed, dehydrated as described in Koskela *et al.* (2018), and gradually embedded over 3 d into Araldite 502/Embed 812 resin (EMS, catalogue no. 13940). The resin was polymerised at 60°C for 48 h. For bright field observation, transverse semithin sections (1 µm) were collected on glass slides, stained with 1% aqueous toluidine blue (TBO) (O'Brien *et al.*, 1964) and supplemented with 1% sodium tetraborate. Samples were imaged with a Zeiss Axio Imager.

Sequence analysis

For protein sequence alignments we used CLUSTAL OMEGA (Madeira *et al.*, 2019). For synteny analysis, we compared the genomic regions containing *AaTOE2* (LT669795.1) and *TOE2* (*AT5G60120*) using the Graphic Alignment Tool for Comparative Sequence Analysis (GATA) plotter (Nix & Eisen, 2005). For phylogenetic analysis, the Maximum Likelihood method based on the JTT matrix-based model (Jones *et al.*, 1992) was used to construct the phylogenetic tree with bootstrapping of 1000 iterations using MEGA7 software (Kumar *et al.*, 2016).

Results

EOP055 is the orthologue of the *AP2*-like gene *TOE2* and represses flowering in *A. alpina* and *Arabidopsis thaliana*

To identify additional genes that regulate flowering and perennial traits in *A. alpina*, we performed an enhancer screen in the *pep1-1* background. The *enhancer of pep1-1 055* (*eop055*) mutant flowered earlier than *pep1-1* in LD and SD glasshouse conditions (Fig. 1a,b). We combined mapping-by-sequencing and classical map-based cloning to identify the causal mutation in *eop005* (Hartwig *et al.*, 2012; Schneeberger, 2014; Andrés *et al.*, 2015).

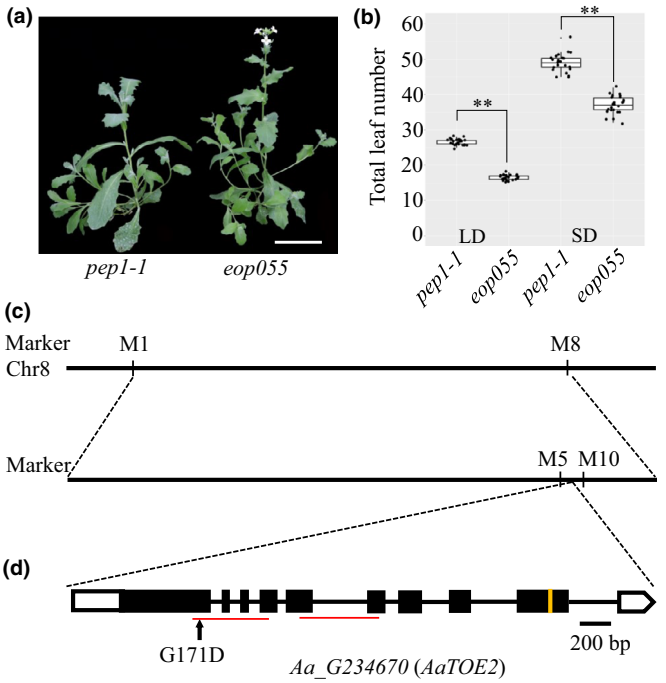

Fig. 1 *Arabis alpina* TOE2 (AaTOE2) is the floral repressor EOP055. (a) Flowering phenotypes of *pep1-1* and *eop055* mutants grown in long days (LDs) for 51 d. (b) Total leaf number at flowering in LDs and short days (SDs). (c) Mapping of *eop055*. The *eop055* mutation was originally mapped using SHOREMAP to the *A. alpina* chromosome 8 between 6 473 171 bp (M1) and 45 736 690 bp (M2). Using fine mapping, the candidate region was narrowed down to a 433 kb genomic region between markers M5 (41 140 691 bp) and M10 (41 574 114 bp). The detailed cloning approach is presented in Fig. S1. (d) Scheme of the *AaTOE2* locus (*Aa_G234670*) showing the position of the mutation and the single nucleotide polymorphism (SNP) found in *eop055*. In (a) bar, 5 cm. In (b) $n = 24$-28. **Indicates significant differences at $P < 0.01$ according to Student's *t*-test. The boxes indicate the interquartile range (IQR), the horizontal line in the middle is the median, the vertical lines (whiskers) correspond to the maximum or minimum value within 1.5 × IQR and the dots are the sample values. In (d) black boxes indicate the exons and white boxes indicate the untranslated regions. Red lines indicate the AP2 domains and the orange line indicates the *miR172* binding site. G171D indicates the nonsynonymous amino acid substitution in the *eop055* mutant from glycine (G) to aspartic acid (D) at amino acid 171. *TOE2*, *TARGET OF EAT 2*; *EOP055*, *ENCHANCER OF PEP1*; *PEP1*, *PERPETUAL FLOWERING 1*.

SHOREMAP analysis indicated that this causal mutation in *eop055* was located in a broad region spanning 40 Mb on the *A. alpina* chromosome 8 (Figs 1c, S1a; Table S2). We reduced the original mapping region (defined between markers M1 and M8) by screening 503 BC1F2 plants with markers designed based on SNPs from SHOREMAP. Fine mapping narrowed down the causal mutation to a 433 kb region (between markers M5 and M10), which contained a single SNP located in the CDS region of the *A. alpina* gene *Aa_G234670* (Figs 1c,d, S1b). Aa_G234670 showed a higher degree of sequence similarity with the AP2-like transcription factor TOE2 in *Arabidopsis thaliana* (Fig. S2). This is one of six *AP2*-like genes in *A. alpina*, the others being (Fig. S2). Synteny of the flanking regions containing *Aa_G234670* and *TOE2* was conserved and *Aa_G234670*

contained a conserved *miR172* binding site (Figs 1d, S3a). Overall, these results suggested that *Aa_G234670* is the orthologue of *TOE2*.

The SNP in *AaTOE2* (*Aa_G234670*) causes a nonsynonymous amino acid substitution from glycine (G) to aspartic acid (D) at amino acid 171 within the first AP2 domain (AP2-R1) (Fig. S3b; Table S2). To verify whether the SNP in *AaTOE2* was responsible for the early flowering phenotype in *eop055*, we complemented the *eop055* mutant using the wild-type 7.8 kb *AaTOE2* genomic region spanning 4128 bp upstream of its translational start and 776 bp downstream of its translational stop. Three independent T3 homozygous lines with a single copy insertion were selected and showed delayed flowering compared with *eop055* (Fig. 2a,b). We also overexpressed the wild-type *AaTOE2* and mutated *Aatoe2* allele in *Arabidopsis thaliana toe2-1*. *AaTOE2* complemented the early flowering phenotype of the *toe2-1* mutant, whereas *Aatoe2* did not (Figs 2c,d, S4). These results suggested that the role of *AaTOE2* in flowering is conserved in *Arabidopsis thaliana* and that the G171D amino acid substitution affects its function. Taken together, these results demonstrate that the *eop055* mutant phenotype was caused by the loss of function of AaTOE2, which represses flowering in *A. alpina* and *Arabidopsis thaliana*.

In *Arabidopsis thaliana*, TOE proteins regulate flowering through the photoperiod pathway (Yant *et al.*, 2009; Zhang *et al.*, 2015). In *A. alpina*, however, the role of the photoperiod pathway in flowering is not very clear and wild-type plants initiate floral buds during cold treatment under SDs (Wang R. *et al.*, 2009). Flowering in response to prolonged cold treatment depends on plant age. Wild-type plants have a juvenile phase of 5 wk so that only plants older than 5 wk are competent to flower in response to prolonged cold treatment (Wang *et al.*, 2011). We found that transcript accumulation of *AaTOE2* in wild-type plants was high in the main shoot apex of vegetative plants and is transiently silenced during cold exposure. However, this is true only for plants that can initiate flowering during cold (adult, 8-wk-old) and not for cold-treated young seedlings (juvenile, 3-wk-old) which remain vegetative (Fig. 3). Transcript accumulation of *AaTOE2* in AMs (within the V3 zone), which also remain vegetative, is similar during and after cold exposure (Fig. 3a). These results suggested AaTOE2 is a floral repressor that is highly expressed in vegetative apices and is differentially regulated spatiotemporally.

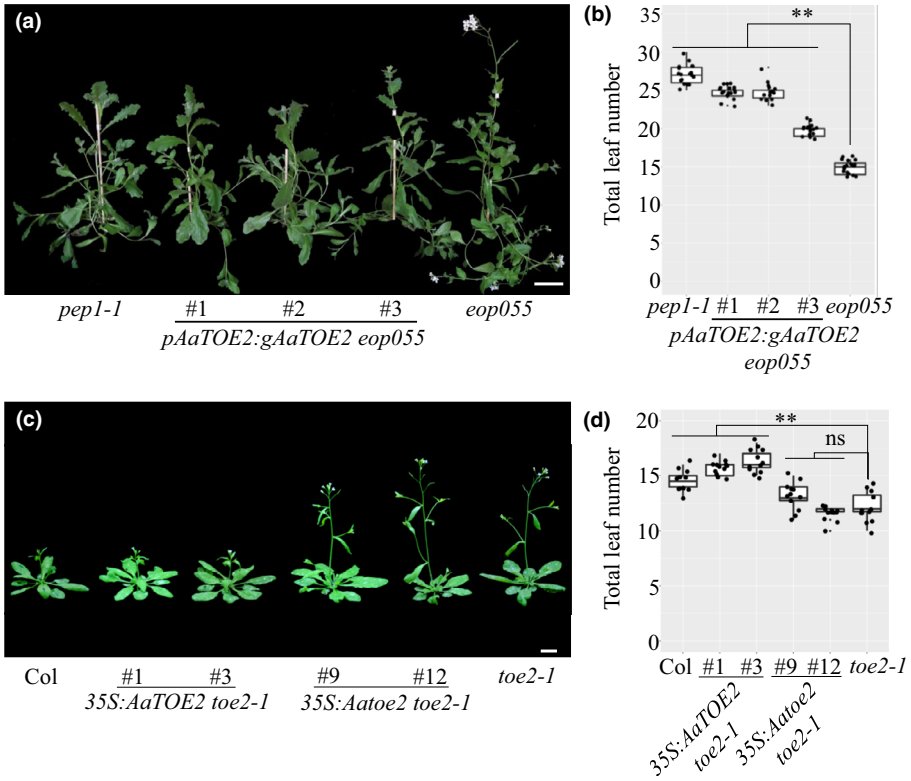

Fig. 2 *AaTOE2* complements the early flowering phenotypes of the *Arabis alpina eop055* and *Arabidopsis thaliana toe2-1* mutants. (a, b) Complementation of *eop055*. (a) Flowering phenotypes of *pep1-1*, *eop055* and three independent *pAaTOE2:gAaTOE2 eop055* transgenic lines grown in long days (LDs) for 57 d. (b) Total leaf number at flowering of *pep1-1*, *eop055* and transgenic lines. (c, d) Complementation of *Arabidopsis thaliana toe2-1* mutant. (c) Flowering phenotypes of Col, *toe2-1* and transgenic lines constitutively expressing the wild-type allele (35S:*AaTOE2*) and mutated allele (35S:*Aatoe2*) of *AaTOE2*. The picture was taken 35 d after sowing in LDs. (d) Total leaf number at bolting of Col, *toe2-1* and transgenic lines in LDs. *AaTOE2* transcript accumulation in *Arabidopsis thaliana* transgenic lines is presented in Supporting Information Fig. S4. Bars: (a) 5 cm; (c) 2 cm. $n = 12$–15. ns, not significant. **Indicates significant differences compared with *eop055* in (b) and *toe2-1* in (d) at $P < 0.01$ according to Student's *t*-test. The boxes and the horizontal line in the middle represent the interquartile range (IQR) and the median, respectively. The whiskers correspond to the maximum or minimum value within 1.5 × IQR, the dots indicate the sample values. *TOE2*, *TARGET OF EAT 2*.

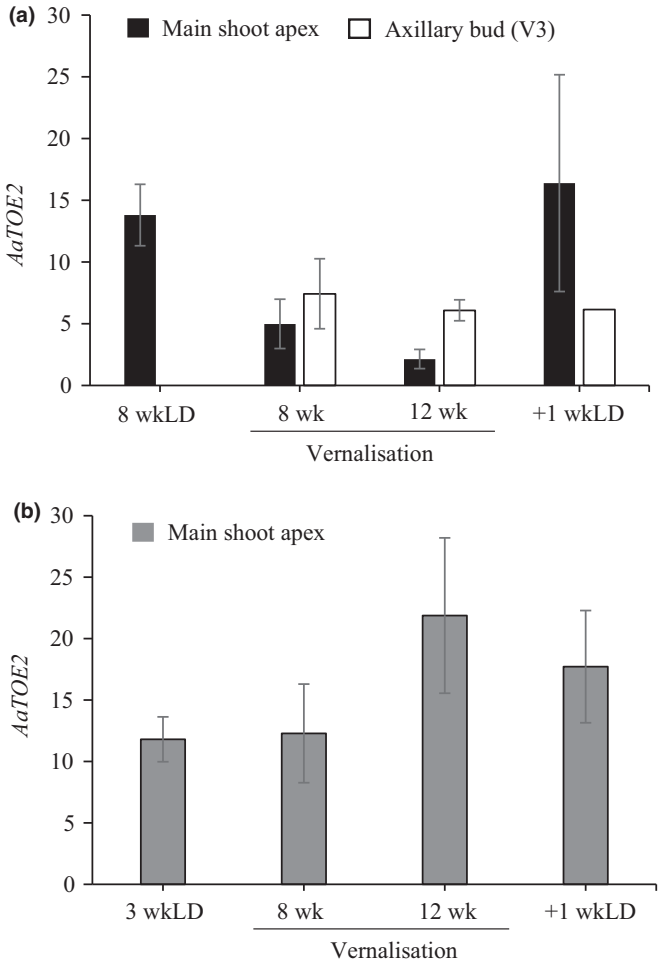

Fig. 3 *AaTOE2* transcript accumulation in wild-type *Arabis alpina* plants differs between meristems and is transiently silenced by cold treatment in a spatial and age-dependent manner. (a) *AaTOE2* mRNA levels in the main shoot apex and subapical axillary buds (V3) of cold-treated 8-wk-old plants. (b) *AaTOE2* mRNA levels in the main shoot apex of cold-treated 3-wk-old plants. The 8-wk-old plants are adult and can initiate flowering in response to vernalisation, whereas 3-wk-old seedlings are juvenile and stay vegetative. Apices/axillary buds were harvested from wild-type plants grown in LD glasshouse conditions after 3 and 8 wk, after cold treatment for 8 and 12 wk and after the return to glasshouse conditions for 1 wk. Error bars represent the standard deviation of three biological replicates. *TOE2*, *TARGET OF EAT 2*.

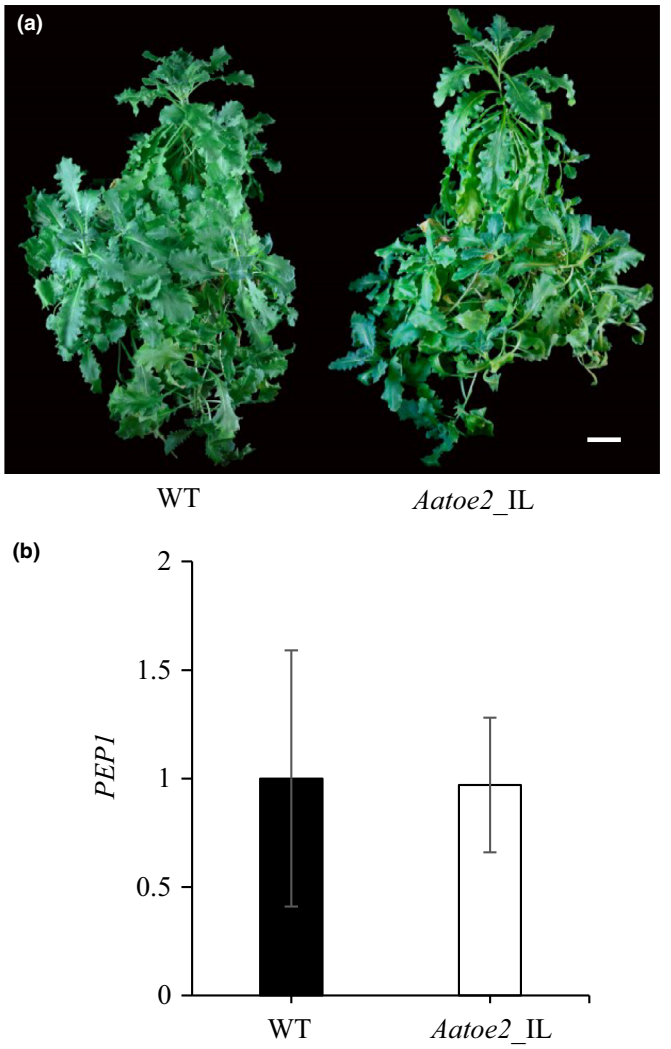

Fig. 4 AaTOE2 in *Arabis alpina* does not regulate flowering through PEP1. (a) Wild-type (WT) and *Aatoe2*_IL plants do not flower after 22 wk in long days (LDs). (b) *PEP1* mRNA levels do not differ between WT and *Aatoe2*_IL 2-wk-old seedlings. Error bars represent the standard deviation of three biological replicates. Bar, 5 cm. *TOE2*, *TARGET OF EAT 2*; *PEP1*, *PERPETUAL FLOWERING 1*.

*Aatoe2*_IL responds to cold treatment at a young age

To understand the function of AaTOE2 in *A. alpina* we introgressed the *Aatoe2* allele into the wild-type background by crossing *eop055* with Pajares and selecting an *Aatoe2*_IL homozygous for *Aatoe2* which contained a functional *PEP1*. We have previously shown that AP2 in *A. alpina* (PEP2) regulates flowering and perennial traits through the age pathway and plays a role in the vernalisation pathway by enhancing *PEP1* mRNA levels (Lázaro *et al.*, 2019). The *pep2-1* mutant does not require cold treatment to flower and has reduced *PEP1* mRNA levels compared with the wild-type (Bergonzi *et al.*, 2013). We checked whether AaTOE2 contributed to the obligate vernalisation requirement of *A. alpina*. We grew *Aatoe2*_IL plants in a LD glasshouse and tested whether they could flower without cold treatment. Similar to the wild-type, *Aatoe2*_IL plants did not flower in LDs (Fig. 4a). *PEP1* mRNA levels also did not differ between 2-wk-old *Aatoe2*_IL and wild-type seedlings (Fig. 4b). This result suggested that AaTOE2 does not regulate flowering through PEP1.

AP2-like genes regulate the juvenile to adult phase change and *TOE2* mRNA levels in *Arabidopsis thaliana* decrease in older plants (Jung *et al.*, 2007; Wang, 2014). We tested *AaTOE2* transcript accumulation in the main shoot apex of plants growing for 2–8 wk in a LD glasshouse without cold treatment. *AaTOE2* transcript accumulation did not decrease as plants became older and resembled the expression patterns of *PEP2* published previously (Fig. S5a; Bergonzi *et al.*, 2013). Transcript accumulation of *PEP1* in apices was similar between wild-type and *Aatoe2*_IL plants at all ages tested confirming again that AaTOE2 does not

regulate flowering through PEP1 (Fig. S5i). Interestingly, *PEP2* mRNA levels were slightly upregulated in *Aatoe2*_IL plants at most time points tested (Fig. S5j). AP2 proteins regulate flowering through several feedback mechanisms to upstream components in the age pathway (Yant *et al.*, 2010). To test whether this is also the case in *A. alpina*, we also analysed the accumulation of *miR156* and some of its target genes (*AaSPL3/4/5*, *AaSPL9/15* and *AaSPL10*) (Figs 5a,b, S5b–f). *miR156* accumulation was similar in both *Aatoe2*_IL and wild-type plants and reduced with plant age (Fig. 5a). Among all genes tested, only the accumulation of *AaSPL5* transcripts differed in an age-dependent pattern between the *Aatoe2*_IL and wild-type (Figs 5b, S5b–f). *AaSPL5* mRNA levels were higher in *Aatoe2*_IL and increased in the apices of older plants (Fig. 5b). In *Arabidopsis thaliana*, *SPL3/4/5* transcript levels are upregulated in transgenic plants constitutively expressing 35S:MIR172b and are increased in double and triple mutants of *AP2*-like genes (Jung *et al.*, 2011). To test whether *miR172* accumulation was also coupled with the changes in *AaSPL5*, we compared *miR172* levels between *Aatoe2*_IL and wild-type plants (Fig. 5c). The results we observed were opposite to what we would have expected based on studies in *Arabidopsis thaliana* and also in comparison with previous findings in *A. alpina* (Jung *et al.*, 2011; Bergonzi *et al.*, 2013). We found that *miR172* accumulation increased with plant age and that in *Aatoe2*_IL it was lower compared with the wild-type (Fig. 5c). This result also correlated with the slight reduction in *PEP2* mRNA levels in *Aatoe2*_IL apices (Fig. S5j). In *Arabidopsis thaliana*, *SPL3/4/5* promote flowering by transcriptionally activating the floral meristem identity genes such as *AP1*, *LFY* and *FUL* in conjunction with the transcription factor FD (Yamaguchi *et al.*, 2009; Wang J.W. *et al.*, 2009a; Jung *et al.*, 2016). In *Aatoe2*_IL plants growing in a LD glasshouse, the expression of meristem identity genes did not differ compared with the wild-type (Fig. S5g,h). These results were in agreement with the fact that *Aatoe2*_IL plants do not flower without cold treatment.

The effect of the age pathway in *A. alpina* is obvious after cold treatment (Wang *et al.*, 2011; Bergonzi *et al.*, 2013; Hyun *et al.*, 2019; Lázaro *et al.*, 2019). To test whether AaTOE2 regulated the age-dependent response to vernalisation, we vernalised 3-wk-old wild-type and *Aatoe2*_IL seedlings for 12 wk and tested whether they flowered (Fig. 5d). *Aatoe2*_IL seedlings flowered in response to cold treatment, whereas wild-type plants did not, suggesting that AaTOE2 regulated the response to vernalisation in an age-dependent manner (Fig. 5d). This result is also in agreement with the age-dependent differences observed in the silencing of *AaTOE2* mRNA levels by cold.

Overall, these results suggested that AaTOE2 regulates the age-dependent response to vernalisation and influences *miR172* and *AaSPL5* mRNA levels at the shoot apical meristem (SAM).

*Aatoe2*_IL has more flowering axillary branches compared to the wild-type

In *A. alpina*, all genes identified so far that regulate the age-dependent response to vernalisation also contribute to the duration of vernalisation required for flowering and determine the fate of

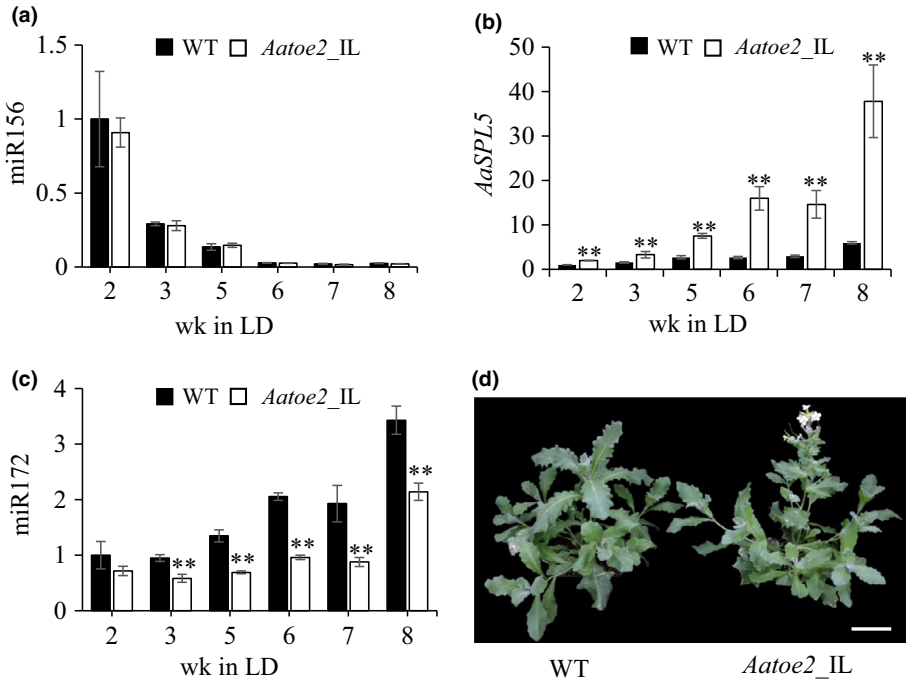

Fig. 5 AaTOE2 in *Arabis alpina* regulates the age-dependent response to cold treatment. (a–c) Expression patterns of (a) *miR156*, (b) *AaSPL5* and (c) *miR172* in apices of wild-type (WT) and *Aatoe2*_IL plants growing for up to 8 wk in a long day (LD) glasshouse. Transcript accumulation of additional genes using the same samples is presented in Supporting Information Fig. S5. (d) Flowering phenotypes of WT and *Aatoe2*_IL plants vernalised at the age of 3 wk. Seedlings were exposed to 12 wk of cold treatment followed by 4 wk in LDs. Error bars represent the standard deviation of three biological replicates. **Indicates significant differences between WT and *Aatoe2*_IL at each time point at $P < 0.01$ according to Student's *t*-test. Bar, 5 cm. *TOE2*, *TARGET OF EAT 2*; *miR156*, microRNA 156, *SPL5*, *SQUAMOSA PROMOTER-BINDING PROTEIN-LIKE 5*; *miR172*, microRNA 172.

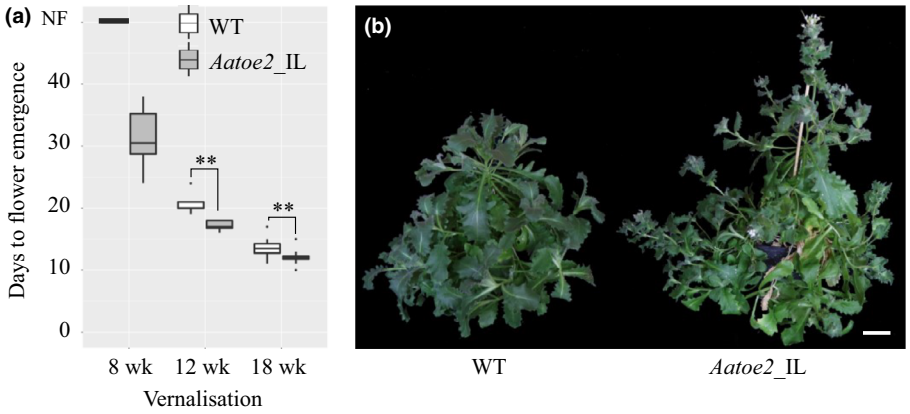

Fig. 6 AaTOE2 extends the duration of cold treatment required for flowering in adult *Arabis alpina* plants. (a) Days to flowering of wild-type (WT) and *Aatoe2*_IL plants exposed to different durations of cold treatment. Flowering time was measured in plants grown for 8 wk in long days (LDs), exposed to 8, 12 or 18 wk of cold treatment and subsequently returned to a LD glasshouse. Days to flowering were counted from the day that plants were transferred to LD glasshouse conditions after vernalisation. (b) Flowering phenotype of WT and *Aatoe2*_IL plants cold-treated for 8 wk, followed by 4 wk in LDs. The boxes indicate the interquartile range (IQR), the horizontal line in the middle is the median, the vertical lines (whiskers) correspond to the maximum or minimum value within 1.5 × IQR and the dots are the outliers. **Indicates significant differences between WT and *Aatoe2*_IL at each cold treatment at $P < 0.01$ according to Student's *t*-test. Bar, 5 cm. $n = 12$. *TOE2*, *TARGET OF EAT 2*.

subapical axillary branches (Wang *et al.*, 2011; Hyun *et al.*, 2019; Lázaro *et al.*, 2019). To test whether this also stands for AaTOE2, we exposed 8-wk-old *Aatoe2*_IL plants to 8, 12 or 18 wk of cold treatment and tested flowering time after transfer to an LD glasshouse. *Aatoe2*_IL plants flowered earlier than wild-type after different durations of cold treatment (Fig. 6a). The biggest effect was observed in plants cold-treated for 8 wk when wild-type plants did not flower but *Aatoe2*_IL plants did (Fig. 6a, b). This result suggested that AaTOE2 regulates the duration of vernalisation required for flowering in *A. alpina*. Interestingly, the shoot apical meristems of wild-type and *Aatoe2*_IL plants were both reproductive at the end of the 8 wk of cold treatment (Fig. S6), suggesting that AaTOE2 antagonises the commitment to flowering after vernalisation.

We also scored shoot architecture in plants exposed to 12 wk of vernalisation, as it was previously shown that this was sufficient to ensure the formation of zones with differential bud activity and fate (Lázaro *et al.*, 2018; Vayssières *et al.*, 2020). As previously published, in wild-type plants the axillary branches at lower leaf nodes (V1) flowered in response to vernalisation and differed from inflorescence branches (I) because they only senesced partially after flowering (Fig. 7b; Wang R. *et al.*, 2009b; Lázaro *et al.*, 2018; Vayssières *et al.*, 2020). Wild-type *A. alpina* plants also maintained a zone of dormant axillary buds (V2) and vegetative axillary branches (V3), which are vital to maintain the perennial life cycle (Lázaro *et al.*, 2018; Vayssières *et al.*, 2020). In *Aatoe2*_IL plants, the axillary branches in the leaf nodes corresponding to the V3 zone flowered (Fig. 7a,b). Flowering V3 branches in *Aatoe2*_IL behaved similarly to V1 branches and partially senesced (Figs 7d,e, S7). Interestingly, *PEP1* mRNA levels in the V3 branches did not differ between wild-type and *Aatoe2*_IL plants, suggesting again that AaTOE2 regulates flowering in parallel to PEP1 (Fig. 7f). Furthermore, we observed a reduced number of V3 axillary branches and an increased number of V1 flowering axillary branches in *Aatoe2*_IL (Fig. 7b,c). This change in the number of metamers dedicated to V1, V2 and V3 zones was specific to the main shoot, as the architecture of the inflorescence was not influenced in *Aatoe2*_IL plants (Figs 7c, S8).

To understand how AaTOE2 regulates flowering in the main shoot and V3 axillary branches, we performed a transcriptome analysis. We exposed 8-wk-old *Aatoe2*_IL and wild-type plants to 4°C for 8 wk to induce flowering (Fig. S6), and dissected their SAM and V3 buds. Principal component analysis (PCA) analysis indicated that the variable explaining most of the variability (PC1) was tissue, which separated the SAM and V3 bud samples, whereas PC2 separated the samples according to their genotype (Fig. 8a). Most differentially expressed genes (DEGs) between genotypes were detected in V3 buds, with 422 genes being differentially expressed in V3 buds compared with 309 genes in the SAM (Fig. 8b; Table S3). In both tissues, GO analysis indicated enrichment in several biological processes, including response to various stresses and regulation of cellular, metabolic and developmental processes (Fig. S9). Several genes involved in stress responses were differentially expressed between *Aatoe2*_IL and the wild-type (Fig. 8c). In the SAM, many genes involved in the reproductive development were upregulated in the *Aatoe2*_IL (e.g. *AP1*, *AGL5* and *DYT1*) (Fig. 8c; Table S3; Alejandra Mandel *et al.*, 1992; Savidge *et al.*, 1995; Zhang *et al.*, 2006). This result suggested that *Aatoe2*_IL initiated flowering during cold treatment earlier than wild-type plants. Among the genes upregulated specifically in the V3 buds of *Aatoe2*_IL, we detected again SPLs (*SPL3*, *4*, *5* and *10*) and also several *TCP* genes (*AaTCP4*, *10*, *24*) known to be involved in leaf growth, flower development, flowering time and jasmonic acid (JA) metabolism (Fig. 8c; Table S3; Wu *et al.*, 2009; Nag *et al.*, 2009; Danisman *et al.*, 2012; Xu *et al.*, 2016; Jung *et al.*, 2016; Lucero *et al.*, 2017; Chang *et al.*, 2018). In the V3 buds, *miR172* accumulation was higher in *Aatoe2*_IL, whereas *miR156* was lower compared with the wild-type (Fig. S10a). These results differed from the *miR172*

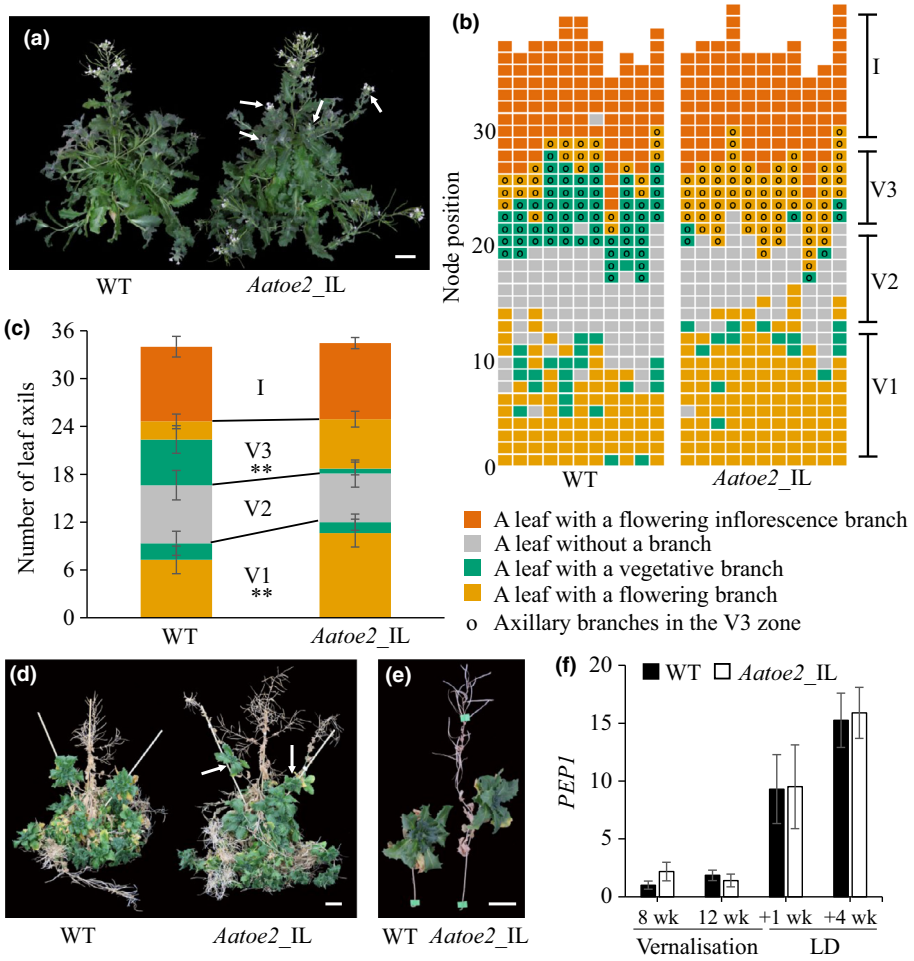

Fig. 7 AaTOE2 regulates shoot architecture in *Arabis alpina* by influencing the number of flowering axillary branches. (a–e) Scoring of plant architecture in wild-type (WT) and *Aatoe2*_IL plants grown for 8 wk in long days (LDs), vernalised for 12 wk and transferred back to an LD glasshouse. (a) Flowering phenotype of vernalised WT and *Aatoe2*_IL plants after they were returned to an LD glasshouse for 4 wk, in which subapical axillary branches in *Aatoe2*_IL plants flowered (*arrows*). (b) Schematic representation of shoot architecture of flowering WT and *Aatoe2*_IL plants. Each column represents a single plant and each box within a column represents a single leaf axil numbered from the bottom to the top of the plant. Different zones are indicated on the right as described for a WT plant in Vayssières *et al.* (2020). V1, flowering axillary branches that partially senesce; V2, dormant buds; V3, vegetative axillary branches; I, inflorescence. Light orange denotes a flowering axillary branch and orange a flowering inflorescence branch. Green represents vegetative axillary branches and grey axillary buds or empty leaf axils. Boxes with circles indicate axillary branches in the V3 zone. (c) Number of leaf axils with or without an axillary flowering/vegetative branch in each zone from (b). (d) Flowering phenotype of vernalised WT and *Aatoe2*_IL plants after they were returned for 20 wk to a LD glasshouse, in which subapical axillary branches in *Aatoe2*_IL plants partially senesced (*arrows*). (e) V3 axillary branches of WT and *Aatoe2*_IL plants that are indicated in (d). V1 axillary branches on the same plants are shown in Supporting Information Fig. S7. Characterisation of inflorescence architecture on the same plants is presented in Fig. S8. (f) Relative expression of *PEP1* in V3 axillary branches of WT and *Aatoe2*_IL plants during and after vernalisation. Bars, 5 cm (a–e). Error bars in (c) and (f) represent the standard deviation. In (c) ** indicates significant differences between WT and *Aatoe2*_IL plants at each zone at $P < 0.01$ according to Student's *t*-test. $n = 11$. *TOE2*, *TARGET OF EAT 2*; *PEP1*, *PERPETUAL FLOWERING 1*.

expression patterns we obtained in the main shoot apex of vegetative plants in a LD glasshouse (Fig. 5c), although *AaSPL5* mRNA levels followed a similar trend and were higher in both vegetative shoot apices and V3 buds of *Aatoe2*_IL plants (Figs 5, S10). V3 buds are formed during vernalisation (Ponraj & Theres, 2020) and therefore can commit to reproductive development if they acquire competence. To check whether V3 buds of *Aatoe2*_IL plants become reproductive during vernalisation, we cold-treated plants for 12 wk and looked at axillary buds in the V3 zone (Fig. S11). In wild-type plants, the axillary buds were vegetative whereas the ones from *Aatoe2*_IL plants had the characteristic dome shape of a flowering meristem (Fig. S11). These results suggested that flowering in V3 buds of *Aatoe2*_IL plants is initiated during vernalisation and that the increase of *miR172* accumulation and *AaSPL5* mRNA levels correlated with the initiation of flowering.

Taken together, these results suggested that *AaTOE2* represses flowering in the SAM and V3 buds during vernalisation.

Initiation rate of AMs and leaves are affected in *Aatoe2*_IL

In *Aatoe2*_IL plants, the number of basal flowering axillary branches (corresponding to V1) was increased (Fig. 7b,c). As V1 axillary branches are formed before cold exposure, we compared

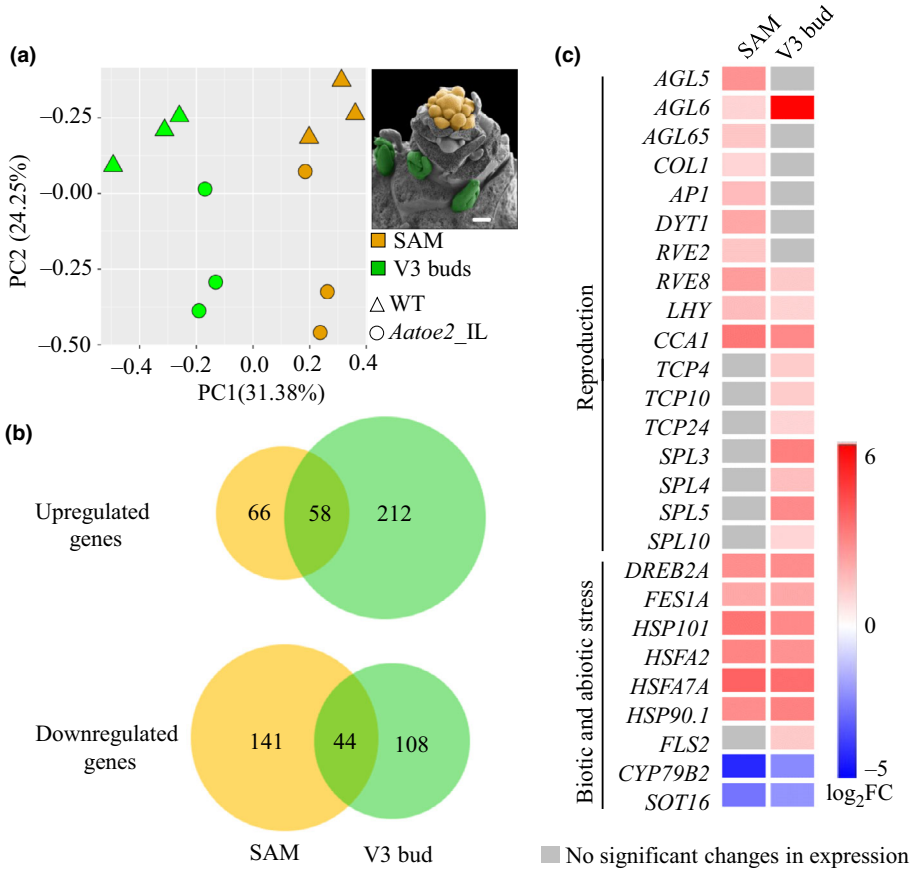

Fig. 8 Bud-specific transcriptome analysis indicates that *AaTOE2* in *Arabis alpina* regulates the expression of *AaSPL3/4/5/10* in subapical axillary buds. (a) Principal component analysis (PCA) of RNA-seq samples. Inset on the right indicates the SAM (yellow) and V3 axillary bud (green) that were harvested for the RNA-seq. (b) Venn diagrams represent the overlap of upregulated and downregulated genes in *Aatoe2*_IL plants compared with the wild-type (WT) in two tissues: the SAM (yellow) and V3 bud (green). (c) Gene expression heatmap of selected differentially expressed genes (DEGs) using the $\log_2$ fold change ($\log_2$FC) values in the SAM and V3 bud samples. All DEGs are listed in Supporting Information Table S3. In the same samples the expression of *miR156*, *miR172*, *AaTOE2* and *AaSPL5* was measured (see Fig. S10). Bar, 100 μm (a). *TOE2*, *TARGET OF EAT 2*; *AGL5*, *AGL6* and *AGL65*, *AGAMOUS-LIKE 5*, *6* and *65*; *COL1*, *CONSTANS-LIKE 1*; *AP1*, *APETALA 1*; *DYT1*, *DYSFUNCTIONAL TAPETUM 1*; *RVE2* and *REV8*, *REVEILLE 2* and *8*; *LHY*, *LATE ELONGATED HYPOCOTYL 1*; *CCA1*, *CIRCADIAN CLOCK ASSOCIATED 1*; *TCP4*, *TCP10* and *TCP24*, *TCP FAMILY TRANSCRIPTION FACTOR 4*, *10* and *24*; *SPL3*, *SPL4*, *SPL5* and *SPL10*, *SQUAMOSA PROMOTER-BINDING PROTEIN-LIKE 3*, *4*, *5* and 10; *DREB2A*, *DRE-BINDING PROTEIN 2A*; *FES1A*, *Factor Exchange for Ssa1p*; *HSP101* and *HSP90.1*; *HEAT SHOCK PROTEIN 101* and *90.1*; *HSFA2* and *HSFA7A*, *HEAT SHOCK TRANSCRIPTION FACTOR A2* and *A7A*; *FLS2*, *FLAGELLIN-SENSITIVE 2*; *CYP79B2*, *CYTOCHROME P450, FAMILY 79, SUBFAMILY B, POLYPEPTIDE 2*; *SOT16*, *SULFOTRANSFERASE 16*.

the number of axillary branches between genotypes before vernalisation (Vayssières *et al.*, 2020). Here, 8-wk-old *Aatoe2*_IL plants had 12.3 ± 2.0 branches compared with the wild-type that had only 7.2 ± 1.2 branches (Figs 9a, S12b). Components of the age pathway regulate other traits, including leaf initiation rate (plastochron) and branching (Wang & Wang, 2015). The *toe2* mutants do not have a clear plastochron phenotype and in 35S:*MIR172b* plants the plastochron is not affected (Jung *et al.*, 2011). Nevertheless, in the triple mutant *spl3/4/5* plastochron is reduced (Jung *et al.*, 2016). We followed leaf initiation in plants grown for up to 8 wk in LDs, and by contrast to the branching phenotype, we detected a statistically significant reduction in the leaf initiation rate in *Aatoe2*_IL plants compared with the wild-type (Fig. S12).

We also had a closer look at the branching phenotype in the *Aatoe2*_IL by scoring the presence or absence of an AM/bud in each leaf node at different developmental stages (Fig. 9b–d). In wild-type plants, it has recently been reported that during vegetative development the leaf axils close to the SAM do not contain an AM (Ponraj & Theres, 2020). These leaf axils fill up during vernalisation when the SAM transitions to reproductive development (Ponraj & Theres, 2020). *Aatoe2*_IL plants have a reduced number of empty leaf axils before and during vernalisation, suggesting that AM initiation is enhanced compared with the wild-type, which results in the increased number of basal axillary branches (Fig. 9e,f). Empty apical leaf axils in plants before vernalisation serve as sites where V3 buds will be formed during cold (Ponraj & Theres, 2020), explaining the reduced number of V3 axillary branches in *Aatoe2*_IL plants (Fig. 9e,g,h).

These results indicated that *AaTOE2* regulates AM formation and shoot architecture in *A. alpina*.

Discussion

In perennials, regrowth from one year to the next is ensured by vegetative axillary or apical meristems. Therefore, perennial

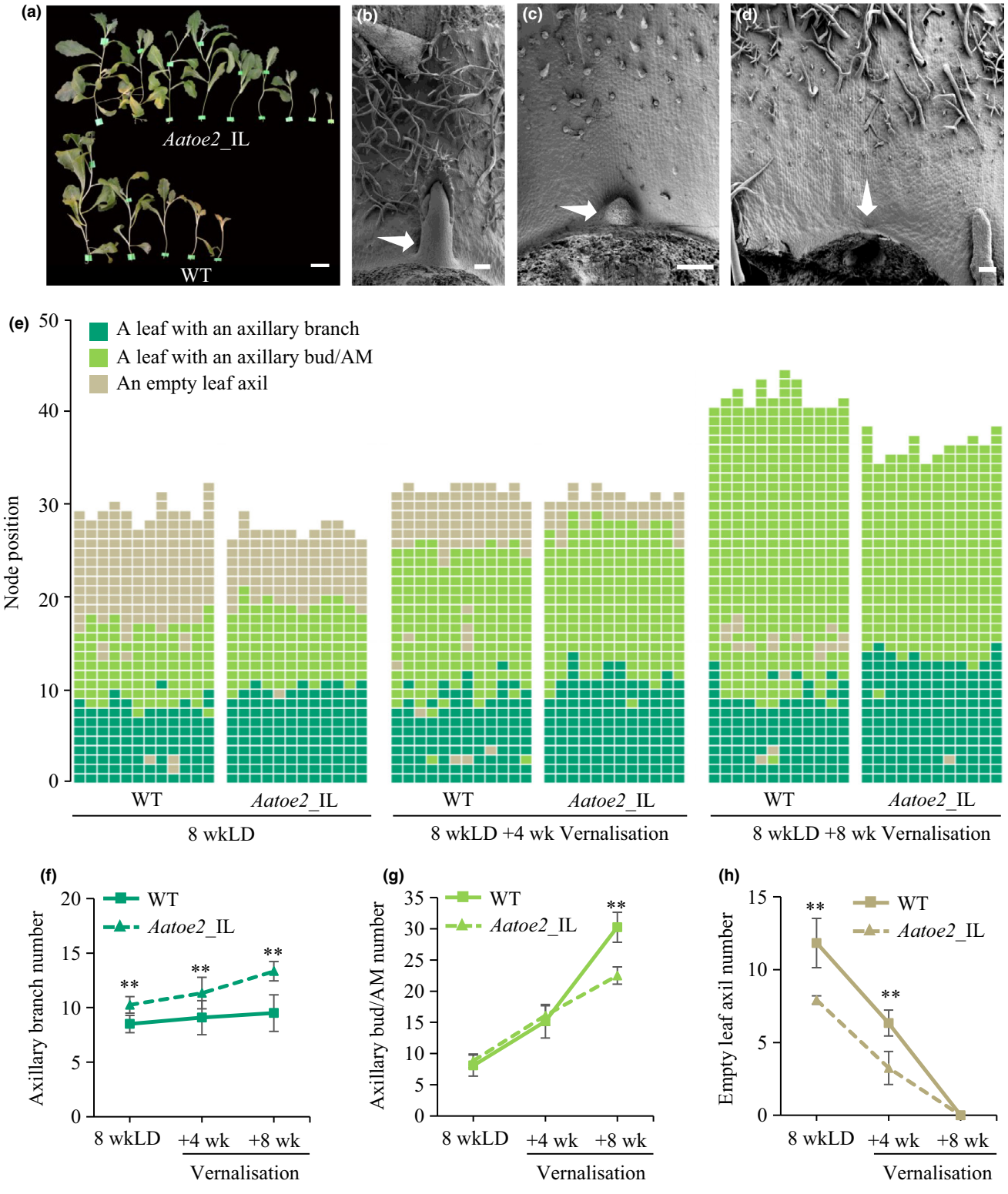

Fig. 9 AaTOE2 enhances the number of apical leaf primordia without an axillary meristem in vegetative *Arabis alpina* plants. (a) Axillary branches in *Aatoe2*_IL and wild-type (WT) plants grown for 8 wk in a long day (LD) glasshouse. (b–d) Scanning electron microscopy (SEM) images of (b) an axillary bud, (c) an axillary meristem (AM) and (d) an empty leaf axil. (e) Schematic representation of axillary bud formation of WT and *Aatoe2*_IL plants grown for 8 wk in an LD glasshouse (8wLD), vernalised for 4 wk or 8 wk. Each column represents a single plant and each box within a column represents a single leaf axil numbered from the bottom to the top of each plant. Green indicates the presence of a branch, light green of an axillary bud/AM and beige of a leaf axil without an AM. (f–h) Number of (f) axillary branches, (g) axillary buds/AMs, (h) leaf axils without an AM in plants presented in (e). **Indicates significant differences between WT and *Aatoe2*_IL plants at each time point at $P < 0.01$ according to Student's *t*-test. Bars: (a) 3 cm; (b–d) 100 μm. In (e) and (f) $n = 12$. Arrows indicate an axillary bud in (b), an axillary meristem in (c) and an empty leaf axil in (d). *TOE2*, *TARGET OF EAT 2*.

species usually show a complex shoot architecture that can consist of dormant buds and axillary vegetative and/or flowering branches (Costes *et al.*, 2014; Vayssières *et al.*, 2020). This strategy of splitting resources towards vegetative and reproductive development affects yield (Bazzaz *et al.*, 1987). Thus, although perennial crops are considered to be the future in sustainable agriculture, they could eventually have a reduced yearly yield compared with established annual crops (Cox *et al.*, 2006). Understanding shoot architecture in perennials can provide us with tools to improve crop yield. In *Arabidopsis thaliana*, the flowering phenotype of mutants such as *toe2* is not very strong due to functional redundancy with other *AP2*-like genes (Aukerman & Sakai, 2003; Jung *et al.*, 2007; Zhai *et al.*, 2015). We describe that in *A. alpina,* although it contains six *AP2*-like genes, the *toe2* mutant has a strong early flowering time phenotype. Thus, we concluded that functional redundancy between *AP2*-like genes might be weaker in *A. alpina*. We also show that AaTOE2 contributed to the polycarpic growth habit by regulating the number and fate of axillary branches that will stay vegetative the following year. This role of AaTOE2 can affect the final yield as it modulates the balance between reproductive and vegetative development. AaTOE2 also controls the vernalisation response by regulating the age at which plants are sensitive to vernalisation as well as the duration of cold required for flowering. Hence, we concluded that AaTOE2 regulates different developmental traits that contribute to the perennial life cycle of *A. alpina*.

AaTOE2 regulates reproductive competence and the duration of cold treatment required for flowering in *A. alpina*

Wild-type Pajares plants flower only if exposed to cold treatment at an age older than 5 wk (Wang *et al.*, 2011; Bergonzi *et al.*, 2013). Similar to other species, in *A. alpina miR156* and members of the SPL and AP2-subfamilies also regulate the competence to flower and determine the age at which plants are able to respond to vernalisation (Bergonzi *et al.*, 2013; Teotia & Tang, 2015; Hyun *et al.*, 2019; Lázaro *et al.*, 2019). Transgenic *A. alpina* lines with reduced *miR156* activity or overexpressing the *miR156*-resistant form of *AaSPL15*, flower when vernalised as young seedlings (grown for 2 or 3 wk before vernalisation) (Bergonzi *et al.*, 2013; Hyun *et al.*, 2019). We demonstrated that *miR172* accumulation increased when *A. alpina* plants became older, resembling previous studies in *Arabidopsis thaliana* and other species, a mechanism regulated by SPL9, SPL10 and SPL3/4/5 (Aukerman & Sakai, 2003; Chuck *et al.*, 2007; Wu *et al.*, 2009; Xie *et al.*, 2020). We also established a role for AaTOE2 in reproductive competence and placed *AaSPL5* downstream of *AaTOE2* (Fig. 10). In *Arabidopsis thaliana SPL3/4/5* mRNA levels are upregulated in plants overexpressing *miR172* and in *toe1 toe2* double or *toe1 toe2 smz* triple mutants (Jung *et al.*, 2011). Thus, it has been suggested that SPL3/4/5 are post-transcriptionally regulated by *miR156* and transcriptionally by *miR172* probably through the *AP2*-like genes (Jung *et al.*, 2011). Our data indicated that in *A. alpina* there are parallel pathways to those described in *Arabidopsis thaliana* and feedback loops influence the expression of SPLs and *miR172*. However, by contrast with *Arabidopsis thaliana*, we detected that AaTOE2 in vegetative shoot apices positively regulates *miR172* accumulation (Yant *et al.*, 2010). SPL3/4/5 induced flowering by binding to the promoters of *APETALA1*, *LEAFY*, and *FRUITFULL* (Yamaguchi *et al.*, 2009; Wang J.W. *et al.*, 2009a; Jung *et al.*, 2016). In our experiments, *A. alpina* plants do not initiate flowering without exposure to cold treatment. The upregulation of *AaSPL5* mRNA in the SAM before cold exposure might be an indicator of enhanced sensitivity to flowering inductive stimuli. AaTOE2 also regulates the duration of cold treatment required to achieve floral

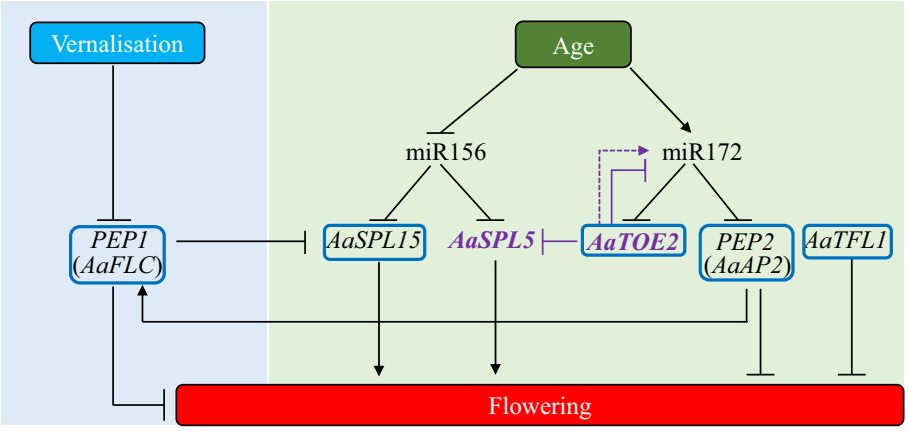

Fig. 10 Schematic diagram showing the network of genes regulating flowering in the perennial *Arabis alpina*. The age and the vernalisation pathways in *A. alpina* are equally important for flowering. *PERPETUAL FLOWERING 1* (*PEP1*), represses flowering through the vernalisation pathway. The *A. alpina* orthologues of *APETALA2* (*PERPETUAL FLOWERING2*, *PEP2*), *SQUAMOSA PROMOTER-BINDING PROTEIN-LIKE15* (*AaSPL15*), *TERMINAL FLOWER1* (*AaTFL1*) and *TARGET OF EAT2 (AaTOE2)* regulate flowering through the age pathway. Most of these genes also regulate other traits related to flowering (blue boxes): (1) The duration of vernalisation required for flowering and the achievement of floral commitment during cold exposure and (2) The fate of axillary branches. In this study, we demonstrated that AaTOE2 also regulates axillary meristem initiation. Genes described in this study are shown in purple. The feedback loop between AaTOE2 and *miR172* (microRNA 172) differs between vegetative (dotted line) and flowering (solid line) meristems.

commitment in cold, which is an important trait for alpine species adapted to environments with short growth seasons (Billings & Mooney, 1968; Aydelotte & Diggle, 1997; Wang R. *et al.*, 2009b; Lázaro *et al.*, 2018). Interestingly, all genes that regulate competence to flower in *A. alpina* also influence the duration of vernalisation required for flowering (Fig. 10). We have previously published that *A. alpina* mutants in floral repressors (e.g. AaTFL1, PEP2) that regulate the age-dependent response to vernalisation also flower after a shorter duration of vernalisation, whereas mutants in floral promoters (e.g. AaSPL15) show strong floral reversion phenotypes after cold exposure (Wang *et al.*, 2011; Bergonzi *et al.*, 2013; Hyun *et al.*, 2019). It is, therefore, very interesting to understand why and how these two traits are associated, especially because transcript accumulation of these genes does not differ between nonvernalised young and old seedlings (Wang *et al.*, 2011; Bergonzi *et al.*, 2013; Hyun *et al.*, 2019). *AP2* and *AP2*-like genes have been mainly studied for traits such as floral development, inflorescence and spikelet architecture (Greenwood *et al.*, 2017; François *et al.*, 2018; Gattolin *et al.*, 2018; Harrop *et al.*, 2019; Debernardi *et al.*, 2020). Similarly, TFL1 and SPL15 have also been reported to play a role in inflorescence architecture in other species (Jiao *et al.*, 2010; Jiang *et al.*, 2013). For AaTOE2, we did not observe a role in inflorescence architecture. However, the fact that the development of floral buds in *A. alpina* occurs during vernalisation may explain the role of AaTOE2 in the duration of vernalisation required for flowering. Our transcriptome analysis also indicated that AaTOE2 may influence how plants modify developmental transitions due to environmental stresses, as previously suggested for other flowering time genes (Riboni *et al.*, 2014; Kazan & Lyons, 2016).

AaTOE2 regulates shoot architecture by inhibiting AM initiation and by repressing flowering in AMs formed during cold treatment

Shoot architecture in *A. alpina* is organised in zones of consequent nodes that behave in a similar way and is determined by the differential response of AMs to cold treatment (Lázaro *et al.*, 2018; Vayssières *et al.*, 2020). We have previously shown that the maintenance of vegetative growth is determined after vernalisation by *PEP1*, whose mRNA levels are upregulated in the subapical axillary branches (V3 branches) to repress flowering (Wang R. *et al.*, 2009b; Lázaro *et al.*, 2018). AMs that will give rise to V3 axillary branches are formed during vernalisation in the axils of the leaf primordia close to the SAM (Ponraj & Theres, 2020). In the *Aatoe2*_IL plants, V3 AMs initiate flowering during cold treatment, suggesting that the fate of these meristems is regulated during vernalisation by AaTOE2. The initiation of flowering in V3 buds was also correlated with a strong increase of *miR172* levels, which differed to our results on the vegetative shoot apices. Thus, the network between different components in the age pathway may vary between vegetative and flowering apices. *AaSPL5,* probably, does not participate in this differential AaTOE2/*miR172* feedback. The *A. alpina* AP2 (PEP2) regulates the fate of V3 branches by ensuring the upregulation of *PEP1* mRNA levels after vernalisation (Lázaro *et al.*, 2019). In this respect, AaTOE2 differs from PEP2 as it does not influence *PEP1* expression levels. Nevertheless, AaTOE2 has an effect on flowering only in vernalised plants suggesting that PEP1 plays a prominent role repressing flowering in parallel to AaTOE2. PEP2 regulates flowering through the age and the vernalisation pathways (Lázaro *et al.*, 2019). Thus, although AaTOE2 does not influence *PEP1* mRNA levels, it could have overlapping functions with PEP2 through the age pathway.

AMs are initiated acropetally at a distance from the SAM and during vegetative development in *Arabidopsis thaliana* and *A. alpina* plants the leaf axils adjacent to the SAM lack an AM (Stirnberg *et al.*, 1999; Reinhardt & Kuhlemeier, 2002; Greb *et al.*, 2003; Ponraj & Theres, 2020). In *Arabidopsis thaliana*, the signal from the SAM that inhibits AM initiation may be auxin, as auxin resistant mutants (*axr1-3* and *axr1-12*) have a reduced number of leaf nodes without an AM (Ponraj & Theres, 2020). Empty leaf axils close to the SAM are filled with an AM soon after *A. alpina* plants are exposed to cold (Ponraj & Theres, 2020). Cold treatment also causes a reduction of endogenous IAA levels in *A. alpina* stems (Vayssières *et al.*, 2020). These results suggested that in *A. alpina* similar mechanisms might contribute to the inhibition and release of growth in the subapical leaf axils. In this study, we observed that *Aatoe2*_IL plants had an enhanced AM initiation rate and a reduced number of leaves without an AM. *TOE2* or other *AP2*-like genes or even their regulator *miR172* have not been reported in *Arabidopsis thaliana* to play a role in AMs initiation and/or to have a branching phenotype (Mathieu *et al.*, 2009; Wu *et al.*, 2009; Yant *et al.*, 2010; Zhai *et al.*, 2015). Nevertheless, *miR156* and the SPLs contribute to branching and this role is also coupled with shortened plastochron lengths, which is again a trait that has not been reported for *AP2*-like genes and *miR172* (Wang & Li, 2008; Schwarz *et al.*, 2008; Jung *et al.*, 2011; Zhou *et al.*, 2013). *OsSPL14*, which is the orthologue of the *Arabidopsis thaliana SPL15*, regulates tiller number in rice (Jiao *et al.*, 2010; Luo *et al.*, 2012). The SPLs in *Arabidopsis thaliana* (specifically SPL9 and SPL15) suppress *LATERAL SUPPRESSOR* (*LAS*) expression, which is a central regulator of AM initiation (Greb *et al.*, 2003; Tian *et al.*, 2014). The *spl9-4 spl15-1* double mutants have accessory buds which is an indicator of *LAS* overexpression (Tian *et al.*, 2014). We observed differences in the number of leaf axils dedicated to V1 and V3 zones in *Aatoe2*_IL plants, which is a consequence of the enhanced AM initiation rate in vegetative plants before being exposed to cold treatment. *Aatoe2*_IL plants had more basal V1 axillary branches and fewer branches dedicated to the V3 zone. This phenotype has not been reported in the *Aaspl15* mutant, suggesting that the role of AaTOE2 in AMs initiation is independent of AaSPL15 (Hyun *et al.*, 2019).

Overall, we demonstrated that AaTOE2 regulates several developmental traits that contribute to the perennial life cycle of *A. alpina*. So far, the *miR156*/SPL module has been described as a regulatory hub due to its conservation in different species and the range of different phenotypes it influences (Wang, 2015;

Wang & Wang, 2015). We propose that *AP2*-like genes will be useful to breed for improved plant architecture and enhanced yield.

Acknowledgements

MCA acknowledges support from the Deutsche Forschungsgemeinschaft (DFG, German Research Foundation) under the Priority Programme 1530 (Flowering time control: from natural variation to crop improvement) and Germany´s Excellence Strategy – EXC 2048/1 – Project ID: 529 390686111. MCA would like to thank George Coupland for hosting her in his group during her DFG-funded temporary position as Principal Investigator, in which time the mutagenesis screen was performed. The authors would like to thank Rainer Franzen, Julia Benecke and Yan Zeng for technical assistance, Ana Lázaro, Evelyn Obeng-Hinneh and Alice Vayssières for useful discussions, Hequan Sun for help with SHOREMAP analysis and Margaret Kox for the critical reading of the manuscript. Open access funding enabled and organized by Projekt DEAL.

Author contributions

YZ and MCA planned and designed the research, MCA did the mutagenesis screen, YZ performed most experiments for the characterisation of the mutant and analysed the data, NVdlT contributed to experiments during the revision process of the manuscript, UN performed the resin embedding, XG performed the RNA-seq analysis, YZ and MCA wrote the manuscript. All authors read and commented on the manuscript.

ORCID

Maria C. Albani https://orcid.org/0000-0002-8215-020X
Xiangchao Gan https://orcid.org/0000-0001-6398-5191
Ulla Neumann https://orcid.org/0000-0001-9200-4209
Natanael Viñegra de la Torre https://orcid.org/0000-0003-3773-6014
Yanhao Zhou https://orcid.org/0000-0002-6009-8447

References

Albani MC, Coupland G. 2010. Comparative analysis of flowering in annual and perennial plants. In: Timmermans MCP ed. *Current topics in developmental biology*. Elsevier Inc. **91**: 323–348.

Alejandra Mandel M, Gustafson-Brown C, Savidge B, Yanofsky MF. 1992. Molecular characterization of the *Arabidopsis* floral homeotic gene *APETALA1*. *Nature* **360**: 273–277.

Amasino R. 2009. Floral induction and monocarpic *versus* polycarpic life histories. *Genome Biology* **10**: 228.

Anders S, Huber W. 2010. Differential expression analysis for sequence count data. *Genome Biology* **11**: R106.

Andrés F, Romera-Branchat M, Martínez-Gallegos R, Patel V, Schneeberger K, Jang S, Altmüller J, Nürnberg P, Coupland G. 2015. Floral induction in Arabidopsis by FLOWERING LOCUS T requires direct repression of *BLADE-ON-PETIOLE* genes by the homeodomain protein PENNYWISE. *Plant Physiology* **169**: 2187–2199.

Aukerman MJ, Sakai H. 2003. Regulation of flowering time and floral organ identity by a microRNA and its *APETALA2*-like target genes. *The Plant Cell* **15**: 2730–2741.

Aydelotte AR, Diggle PK. 1997. Analysis of developmental preformation in the alpine herb *Caltha leptosepala* (Ranunculaceae). *American Journal of Botany* **84**: 1646–1657.

Bazzaz FA, Chiariello NR, Coley PD, Pitelka LF. 1987. Allocating Resources to Reproduction and Defense. *BioScience* **37**: 58–67.

Bergonzi S, Albani MC, Loren Ver, van Themaat E, Nordstrom KJ, Wang R, Schneeberger K, Moerland PD, Coupland G. 2013. Mechanisms of age-dependent response to winter temperature in perennial flowering of *Arabis alpina*. *Science* **340**: 1094–1097.

Billings WD, Mooney HA. 1968. The ecology of arctic and alpine plants. *Biological Reviews* **43**: 481–529.

Chang SH, Tan CM, Wu CT, Lin TH, Jiang SY, Liu RC, Tsai MC, Su LW, Yang JY. 2018. Alterations of plant architecture and phase transition by the phytoplasma virulence factor SAP11. *Journal of Experimental Botany* **69**: 5389–5401.

Chuck G, Cigan AM, Saeteurn K, Hake S. 2007. The heterochronic maize mutant *Corngrass1* results from overexpression of a tandem microRNA. *Nature Genetics* **39**: 544–549.

Clough SJ, Bent AF. 1998. Floral dip: a simplified method for Agrobacterium-mediated transformation of *Arabidopsis thaliana*. *The Plant Journal* **16**: 735–743.

Costes E, Crespel L, Denoyes B, Morel P, Demene MN, Lauri PE, Wenden B. 2014. Bud structure, position and fate generate various branching patterns along shoots of closely related Rosaceae species: a review. *Frontiers in Plant Science* **5**: 666.

Cox TS, Glover JD, Van Tassel DL, Cox CM, DeHaan LR. 2006. Prospects for developing perennial grain crops. *BioScience* **56**: 649–659.

Danisman S, van der Wal F, Dhondt S, Waites R, de Folter S, Bimbo A, van Dijk ADJ, Muino JM, Cutri L, Dornelas MC *et al.* 2012. Arabidopsis class I and class II TCP transcription factors regulate jasmonic acid metabolism and leaf development antagonistically. *Plant Physiology* **159**: 1511–1523.

Debernardi JM, Greenwood JR, Jean Finnegan E, Jernstedt J, Dubcovsky J. 2020. *APETALA 2*-like genes *AP2L2* and *Q* specify lemma identity and axillary floral meristem development in wheat. *The Plant Journal* **101**: 171–187.

Dobin A, Davis CA, Schlesinger F, Drenkow J, Zaleski C, Jha S, Batut P, Chaisson M, Gingeras TR. 2013. STAR: ultrafast universal RNA-seq aligner. *Bioinformatics* **29**: 15–21.

Fortino V, Alenius H, Greco D. 2015. BACA: bubble chArt to compare annotations. *BMC Bioinformatics* **16**: 37.

François L, Verdenaud M, Fu X, Ruleman D, Dubois A, Vandenbussche M, Bendahmane A, Raymond O, Just J, Bendahmane M. 2018. A miR172 target-deficient AP2-like gene correlates with the double flower phenotype in roses. *Scientific Reports* **8**: 12912.

Gao R, Wang Y, Gruber MY, Hannoufa A. 2018. miR156/SPL10 modulates lateral root development, branching and leaf morphology in Arabidopsis by silencing *AGAMOUS-LIKE 79*. *Frontiers in Plant Science* **8**: 2226.

Gattolin S, Cirilli M, Pacheco I, Ciacciulli A, Da Silva Linge C, Mauroux JB, Lambert P, Cammarata E, Bassi D, Pascal T *et al.* 2018. Deletion of the miR172 target site in a TOE-type gene is a strong candidate variant for dominant double-flower trait in Rosaceae. *The Plant Journal* **96**: 358–371.

Greb T, Clarenz O, Schafer E, Muller D, Herrero R, Schmitz G, Theres K. 2003. Molecular analysis of the LATERAL SUPPRESSOR gene in Arabidopsis reveals a conserved control mechanism for axillary meristem formation. *Genes & Development* **17**: 1175–1187.

Greenwood JR, Finnegan EJ, Watanabe N, Trevaskis B, Swain SM. 2017. New alleles of the wheat domestication gene *Q* reveal multiple roles in growth and reproductive development. *Development* **144**: 1959–1965.

Harrop TWR, Mantegazza O, Luong AM, Béthune K, Lorieux M, Jouannic S, Adam H. 2019. A set of *AP2*-like genes is associated with inflorescence branching and architecture in domesticated rice. *Journal of Experimental Botany* **70**: 5617–5629.

Hartwig B, James GV, Konrad K, Schneeberger K, Turck F. 2012. Fast isogenic mapping-by-sequencing of ethyl methanesulfonate-induced mutant bulks. *Plant Physiology* **160**: 591–600.

Huang DW, Sherman BT, Lempicki RA. 2008. Systematic and integrative analysis of large gene lists using DAVID bioinformatics resources. *Nature Protocols* **4**: 44–57.

Hyun Y, Vincent C, Tilmes V, Bergonzi S, Kiefer C, Richter R, Martinez-Gallegos R, Severing E, Coupland G. 2019. A regulatory circuit conferring varied flowering response to cold in annual and perennial plants. *Science* **363**: 409–412.

Jiang K, Liberatore KL, Park SJ, Alvarez JP, Lippman ZB. 2013. Tomato yield heterosis is triggered by a dosage sensitivity of the florigen pathway that fine-tunes shoot architecture. *PLoS Genetics* **9**: e1004043.

Jiao W-B, Accinelli GG, Hartwig B, Kiefer C, Baker D, Severing E, Willing E-M, Piednoel M, Woetzel S, Madrid-Herrero E *et al.* 2017. Improving and correcting the contiguity of long-read genome assemblies of three plant species using optical mapping and chromosome conformation capture data. *Genome Research* **27**: 778–786.

Jiao Y, Wang Y, Xue D, Wang J, Yan M, Liu G, Dong G, Zeng D, Lu Z, Zhu X *et al.* 2010. Regulation of *OsSPL14* by OsmiR156 defines ideal plant architecture in rice. *Nature Genetics* **42**: 541–544.

Jones DT, Taylor WR, Thornton JM. 1992. The rapid generation of mutation data matrices from protein sequences. *Computer Applications in the Biosciences* **8**: 275–282.

Jung JH, Lee HJ, Ryu JY, Park CM. 2016. SPL3/4/5 integrate developmental aging and photoperiodic signals into the FT-FD module in *Arabidopsis* flowering. *Molecular Plant* **9**: 1647–1659.

Jung JH, Seo PJ, Kang SK, Park CM. 2011. miR172 signals are incorporated into the miR156 signaling pathway at the *SPL3/4/5* genes in *Arabidopsis* developmental transitions. *Plant Molecular Biology* **76**: 35–45.

Jung JH, Seo YH, Seo PJ, Reyes JL, Yun J, Chua NH, Park CM. 2007. The *GIGANTEA*-regulated microRNA172 mediates photoperiodic flowering independent of *CONSTANS* in *Arabidopsis*. *The Plant Cell* **19**: 2736–2748.

Kazan K, Lyons R. 2016. The link between flowering time and stress tolerance. *Journal of Experimental Botany* **67**: 47–60.

Klock HE, Koesema EJ, Knuth MW, Lesley SA. 2008. Combining the polymerase incomplete primer extension method for cloning and mutagenesis with microscreening to accelerate structural genomics efforts. *Proteins* **71**: 982–994.

Koskela MM, Brünje A, Ivanauskaite A, Grabsztunowicz M, Lassowskat I, Neumann U, Dinh TV, Sindlinger J, Schwarzer D, Wirtz M *et al.* 2018. Chloroplast acetyltransferase NSI is required for state transitions in *Arabidopsis thaliana*. *The Plant Cell* **30**: 1695–1709.

Kumar S, Stecher G, Tamura K. 2016. MEGA7: molecular evolutionary genetics analysis version 7.0 for bigger datasets. *Molecular Biology and Evolution* **33**: 1870–1874.

Langmead B, Salzberg SL. 2012. Fast gapped-read alignment with Bowtie 2. *Nature Methods* **9**: 357–359.

Lazaro A, Obeng-Hinneh E, Albani MC. 2018. Extended vernalization regulates inflorescence fate in *Arabis alpina* by stably silencing *PERPETUAL FLOWERING1*. *Plant Physiology* **176**: 2819–2833.

Lazaro A, Zhou Y, Giesguth M, Nawaz K, Bergonzi S, Pecinka A, Coupland G, Albani MC. 2019. *PERPETUAL FLOWERING2* coordinates the vernalization response and perennial flowering in *Arabis alpina*. *Journal of Experimental Botany* **70**: 949–961.

Li H, Handsaker B, Wysoker A, Fennell T, Ruan J, Homer N, Marth G, Abecasis G, Durbin R. 2009. The sequence alignment/map format and SAMtools. *Bioinformatics* **25**: 2078–2079.

Lucero LE, Manavella PA, Gras DE, Ariel FD, Gonzalez DH. 2017. Class I and class II TCP transcription factors modulate SOC1-dependent flowering at multiple levels. *Molecular Plant* **10**: 1571–1574.

Luo L, Li W, Miura K, Ashikari M, Kyozuka J. 2012. Control of tiller growth of rice by *OsSPL14* and strigolactones, which work in two independent pathways. *Plant and Cell Physiology* **53**: 1793–1801.

Madeira F, Park YM, Lee J, Buso N, Gur T, Madhusoodanan N, Basutkar P, Tivey ARN, Potter SC, Finn RD *et al.* 2019. The EMBL-EBI search and sequence analysis tools APIs in 2019. *Nucleic Acids Research* **47**: W636–W641.

Mathieu J, Yant LJ, Mürdter F, Küttner F, Schmid M. 2009. Repression of flowering by the miR172 target SMZ. *PLoS Biology* **7**: e1000148.

Michaels SD, Amasino RM. 1999. FLOWERING LOCUS C encodes a novel MADS domain protein that acts as a repressor of flowering. *The Plant Cell* **11**: 949–956.

Nag A, King S, Jack T. 2009. miR319a targeting of *TCP4* is critical for petal growth and development in *Arabidopsis*. *Proceedings of the National Academy of Sciences, USA* **106**: 22534–22539.

Nix DA, Eisen MB. 2005. GATA: A graphic alignment tool for comparative sequence analysis. *BMC Bioinformatics* **25**: 2078–2079.

O'Brien TP, Feder N, McCully ME. 1964. Polychromatic staining of plant cell walls by toluidine blue O. *Protoplasma* **59**: 368–373.

Park J-Y, Kim H, Lee I. 2017. Comparative analysis of molecular and physiological traits between perennial *Arabis alpina* Pajares and annual *Arabidopsis thaliana* Sy-0. *Scientific Reports* **7**: 13348.

Ponraj U, Theres K. 2020. Keep a distance to be different: axillary buds initiating at a distance to the shoot apical meristem are crucial for the perennial life style of *Arabis alpina*. *New Phytologist* **227**: 116–131.

Reinhardt D, Kuhlemeier C. 2002. Plant architecture. *EMBO Reports* **3**: 846–851.

Riboni M, Robustelli Test A, Galbiati M, Tonelli C, Conti L. 2014. Environmental stress and flowering time. *Plant Signaling & Behavior* **9**: 7.

Savidge B, Rounsley SD, Yanofsky MF. 1995. Temporal relationship between the transcription of two Arabidopsis MADS box genes and the floral organ identity genes. *The Plant Cell* **7**: 721–733.

Schneeberger K. 2014. Using next-generation sequencing to isolate mutant genes from forward genetic screens. *Nature Reviews Genetics* **15**: 662–676.

Schneeberger K, Ossowski S, Lanz C, Juul T, Petersen AH, Nielsen KL, Jørgensen J-E, Weigel D, Andersen SU. 2009. SHOREmap: simultaneous mapping and mutation identification by deep sequencing. *Nature Methods* **6**: 550–551.

Schwarz S, Grande AV, Bujdoso N, Saedler H, Huijser P. 2008. The microRNA regulated SBP-box genes *SPL9* and *SPL15* control shoot maturation in Arabidopsis. *Plant Molecular Biology* **67**: 183–195.

Sheldon CC, Rouse DT, Finnegan EJ, Peacock WJ, Dennis ES. 2000. The molecular basis of vernalization: The central role of FLOWERING LOCUS C (FLC). *Proceedings of the National Academy of Sciences, USA* **97**: 3753–3758.

Stirnberg P, Chatfield SP, Leyser HMO. 1999. *AXR1* acts after lateral bud formation to inhibit lateral bud growth in Arabidopsis. *Plant Physiology* **121**: 839–847.

Sun H, Schneeberger K. 2015. SHOREmap v3.0: fast and accurate identification of causal mutations from forward genetic screens. In: Alonso J, Stepanova A, eds. *Plant functional genomics. methods in molecular biology*. New York, NY, USA: Humana Press, **1284**: 381–395.

Tan F, Swain SM. 2006. Genetics of flower initiation and development in annual and perennial plants. *Physiologia Plantarum* **128**: 8–17.

Teotia S, Tang G. 2015. To bloom or not to bloom: role of microRNAs in plant flowering. *Molecular Plant* **8**: 359–377.

Tian C, Zhang X, He J, Yu H, Wang Y, Shi B, Han Y, Wang G, Feng X, Zhang C *et al.* 2014. An organ boundary-enriched gene regulatory network uncovers regulatory hierarchies underlying axillary meristem initiation. *Molecular Systems Biology* **10**: 755.

Vayssières A, Mishra P, Roggen A, Neumann U, Ljung K, Albani MC. 2020. Vernalization shapes shoot architecture and ensures the maintenance of dormant buds in the perennial *Arabis alpina*. *New Phytologist* **227**: 99–115.

Wang H, Wang H. 2015. The miR156/SPL module, a regulatory hub and versatile toolbox, gears up crops for enhanced agronomic traits. *Molecular Plant* **8**: 677–688.

Wang JW. 2014. Regulation of flowering time by the miR156-mediated age pathway. *Journal of Experimental Botany* **65**: 4723–4730.

Wang JW. 2015. The multifaceted roles of miR156-targeted SPL transcription factors in plant developmental transitions. In: Gonzalez DH, ed. *Plant transcription factors: evolutionary, structural and functional aspects*. Amsterdam, the Netherlands: Elsevier, 281–293.

Wang JW, Czech B, Weigel D. 2009. miR156-regulated SPL transcription factors define an endogenous flowering pathway in *Arabidopsis thaliana*. *Cell* **138**: 738–749.

Wang JW, Schwab R, Czech B, Mica E, Weigel D. 2008. Dual effects of miR156-targeted *SPL* genes and *CYP78A5/KLUH* on plastochron length and organ size in *Arabidopsis thaliana*. *The Plant Cell* **20**: 1231–1243.

Wang R, Albani MC, Vincent C, Bergonzi S, Luan M, Bai Y, Kiefer C, Castillo R, Coupland G. 2011. Aa *TFL1* confers an age-dependent response to vernalization in perennial *Arabis alpina*. *The Plant Cell* **23**: 1307–1321.

Wang R, Farrona S, Vincent C, Joecker A, Schoof H, Turck F, Alonso-Blanco C, Coupland G, Albani MC. 2009. *PEP1* regulates perennial flowering in *Arabis alpina*. *Nature* **459**: 423–427.

Wang Y, Li J. 2008. Molecular basis of plant architecture. *Annual Review of Plant Biology* **59**: 253–279.

Wu G, Park MY, Conway SR, Wang JW, Weigel D, Poethig RS. 2009. The sequential action of miR156 and miR172 regulates developmental timing in *Arabidopsis*. *Cell* **138**: 750–759.

Xie Y, Zhou Q, Zhao Y, Li Q, Liu Y, Ma M, Wang B, Shen R, Zheng Z, Wang H. 2020. FHY3 and FAR1 integrate light signal with the miR156-SPL module-mediated aging pathway to regulate *Arabidopsis* flowering. *Molecular Plant* **13**: 483–498.

Xu M, Hu T, Zhao J, Park MY, Earley KW, Wu G, Yang L, Poethig RS. 2016. Developmental functions of miR156-regulated *SQUAMOSA PROMOTER BINDING PROTEIN-LIKE* (*SPL*) genes in *Arabidopsis thaliana*. *PLoS Genetics* **12**: e1006263.

Yamaguchi A, Wu MF, Yang L, Wu G, Poethig RS, Wagner D. 2009. The MicroRNA-regulated SBP-box transcription factor SPL3 is a direct upstream activator of *LEAFY*, *FRUITFULL*, and *APETALA1*. *Developmental Cell* **17**: 268–278.

Yant L, Mathieu J, Dinh TT, Ott F, Lanz C, Wollmann H, Chen X, Schmid M. 2010. Orchestration of the floral transition and floral development in *Arabidopsis* by the bifunctional transcription factor APETALA2. *The Plant Cell* **22**: 2156–2170.

Yant L, Mathieu J, Schmid M. 2009. Just say no: floral repressors help Arabidopsis bide the time. *Current Opinion in Plant Biology* **12**: 580–586.

Zhai Q, Zhang X, Wu F, Feng H, Deng L, Xu L, Zhang M, Wang Q, Li C. 2015. Transcriptional mechanism of jasmonate receptor COI1-mediated delay of flowering time in Arabidopsis. *The Plant Cell* **27**: 2814–2828.

Zhang B, Wang L, Zeng L, Zhang C, Ma H. 2015. Arabidopsis TOE proteins convey a photoperiodic signal to antagonize CONSTANS and regulate flowering time. *Genes & Development* **29**: 975–987.

Zhang W, Sun Y, Timofejeva L, Chen C, Grossniklaus U, Ma H. 2006. Regulation of *Arabidopsis* tapetum development and function by *DYSFUNCTIONAL TAPETUM1* (*DYT1*) encoding a putative bHLH transcription factor. *Development* **133**: 3085–3095.

Zhou CM, Zhang TQ, Wang X, Yu S, Lian H, Tang H, Feng ZY, Zozomova-Lihová J, Wang JW. 2013. Molecular basis of age-dependent vernalization in *Cardamine flexuosa*. *Science* **340**: 1097–1100.

Supporting Information

Additional Supporting Information may be found online in the Supporting Information section at the end of the article.

Fig. S1 Cloning of the *eop055* mutant.

Fig. S2 Phylogenetic relationship of the AP2-like family in *Arabis alpina* and *Arabidopsis thaliana*.

Fig. S3 *Aa_G234670* is the *Arabis alpina* orthologue of *TOE2*.

Fig. S4 *AaTOE2* is constitutively expressed in *Arabidopsis thaliana toe2-1* complementation lines.

Fig. S5 Transcript accumulation of several flowering time regulators does not differ between *Arabis alpina* wild-type and *Aatoe2*_IL plants grown in continuous long day conditions.

Fig. S6 Scanning electron microscopy images of the main shoot apex from wild-type and *Aatoe2*_IL plants vernalised for 8 wk.

Fig. S7 V1 axillary branches of vernalised *Arabis alpina* wild-type and *Aatoe2*_IL plants after they were returned for 20 wk to a long day glasshouse.

Fig. S8 Inflorescence architecture of *Arabis alpina* is not influenced in *Aatoe2*_IL plants.

Fig. S9 Gene ontology enrichment analysis of differentially expressed genes detected between wild-type and *Aatoe2*_IL plants in two different tissues: the main shoot apical meristem and V3 axillary buds.

Fig. S10 Transcript accumulation of *AaTOE2*, *AaSPL5*, *miR172* and *miR156* in V3 buds of *Arabis alpina* wild-type and *Aatoe2*_IL plants.

Fig. S11 V3 buds in *Arabis alpina Aatoe2*_IL plants transitioned to flowering during vernalisation.

Fig. S12 Plastochron and number of axillary branches are increased in *Arabis alpina Aatoe2*_IL plants.

Table S1 Primers used in this study.

Table S2 List of single nucleotide polymorphism within coding sequence regions in chromosome 8 for the *Arabis alpina eop055* mutant.

Table S3 DEGs between *Aatoe2*_IL and wild-type in the main shoot apical meristem and V3 buds.

Please note: Wiley Blackwell are not responsible for the content or functionality of any supporting information supplied by the authors. Any queries (other than missing material) should be directed to the *New Phytologist* Central Office.